*Article*

# Analytical Insights Into the Spread of an Epidemic through Joint Modeling of Disease Dynamics and Attitudes towards Prophylactic Measures and Vaccines

**Chénangnon Frédéric Tovissodé [1,2]* and Romain Glèlè Kakaï [1]**

[1] Laboratoire de Biomathématiques et d'Estimations Forestières, Université d'Abomey-Calavi, Abomey-Calavi, Benin;
[2] Institute for Modeling Collaboration and Innovation, University of Idaho, Moscow, ID, United States
* Correspondence: chenangnon@gmail.com (C.F.T.)

**Abstract:** In this age of mass media and, in particular, social media-driven perception of reality, coupling disease and prophylactic opinion dynamics models can provide better insights into disease evolution than using a disease model alone. We develop in this work two disease-opinion dynamics models based on the epidemiology of the new coronavirus disease (COVID-19) and the availability or not of imperfect vaccines. We assume that susceptibility to infection decreases with the level of prophylactic attitude (personal hygiene, social distancing), and changes in prophylactic attitudes of susceptible individuals occur in response to perceived disease prevalence and vaccination coverage and efficacy in the population. We derive and discuss the disease-free equilibriums and reproduction numbers in the introduced models. We further assess the impacts of the distribution of opinions at disease introduction, the ability to detect presymptomatic, asymptomatic and symptomatic positive COVID-19 cases, the behavioural responses to the outbreak and the introduction of vaccination, and the effects of distortions of disease prevalence by public policy and mass media on disease dynamics. The insights highlighted from the proposed models are expected to make informative contributions to public policy in a context of opinion fluxes in response to perceived disease prevalence.

**Keywords:** COVID-19; Disease-behaviour dynamics model; Prophylactic attitude; Vaccination; Perceived disease prevalence

## 1. Introduction

The emergence in late 2019 of the new coronavirus disease (COVID-19) caused by the pathogen SARS-CoV-2 is an example of highly contagious emerging infectious diseases in response to increases in the magnitude and rate of overexploitation, habitat loss, global loss of biodiversity and climate change that many studies have warned against during the last decades [1–4]. The COVID-19 pandemic has impacted social and cultural habits, recreational and economic activities, laws and rights, among other aspects of human civilization. Increases in personal hygiene and social distancing from perceived sources of infection have shown significant potential to reduce the transmission and, thereby, the spread of COVID-19. But the spread of a contagious disease in this era of mass media and highly connected populations is inevitably concomitant with the dissemination of antagonist information and opinions on the related pathogen, disease, and prophylactic measures [5–8].

Modeling disease dynamics is the unique route to circumventing, containing, anticipating, and preventing or reducing the ravages of deadly emerging or re-emerging infectious diseases. The numerous recent epidemic outbreaks (e.g., MERS, SARS, Ebola) have indeed urged the development of mathematical and statistical models for the spread dynamics of particular diseases. Many such models include opinions regarding vaccination [9–11]. Indeed, vaccines' safety and use have always and everywhere raised controversial issues [12–14]. For instance, controversies about COVID-19 vaccines have been widely spread once the safety and effectiveness assessment trials started, especially in highly connected social networks [15–20]. The opinions and the related attitudes toward vaccines have obvious consequences in the spread of diseases and their ability to cause epidemics [21]. However,

 doi:10.20944/preprints202212.0067.v1



opinions on other prophylactic measures have been less considered, although they can directly impact transmission dynamics and attitudes toward vaccination. In the COVID-19 pandemic context, the dynamics of these other prophylactic behaviours can substantively differ from the dynamics of attitudes toward vaccination [22].

The recent development of models coupling disease, economic and opinion dynamics [23–36] provides headways towards effective joint modeling of health-related beliefs and attitudes, economic constraints, disease dynamics, and their interactions. However, most of the current models primarily rely on quite simplistic assumptions such as the SIS [23,37], SIR [22,38–40] and SEIV models [41] for disease dynamics. For instance, the world's reactions to the COVID-19 outbreaks generally involved isolating some infectious individuals from the susceptible population, making the distinction of "quarantined" individuals from other infectious individuals crucial for sound modeling of this disease [42]. In addition, the epidemiology of COVID-19 indicates even more complex disease dynamics involving presymptomatic, asymptomatic, and symptomatic infectious states [43–50]. In such situations, using too simplistic models can neglect crucial characteristics of target diseases and confound some distinct disease-opinion interactions important for decision-making.

To tackle this background, this study proposes (1) a disease-opinion dynamics model that accounts for basic prophylactic measures against emerging infectious diseases, the related beliefs and behaviours, and important disease states based on COVID-19 epidemiology, and (2) a joint model integrating attitudes toward vaccination and other prophylactic measures with disease dynamics. The objectives of the work are (i) to determine the disease-free and endemic equilibria and the reproduction numbers of the disease-opinion dynamics models, and (ii) to assess the impacts of the initial distribution of behaviours, nature of behavioural responses, vaccination rate and efficacy, rates of detection and isolation ("quarantining"), and perceived disease prevalence on disease dynamics. The use of the proposed models is expected to make informative contributions to public policy in a context of opinion fluxes in response to perceived disease prevalence.

## 2. The Disease-Opinion Dynamics Models

We develop a generalization of the SIR–Opinion dynamics model [22] to suit the epidemiology of the pathogen SARS-CoV-2, the related coronavirus disease (COVID-19), and the availability of imperfect COVID-19 vaccines. On the one hand, we consider a disease evolution model distinguishing the infectious population into presymptomatic, asymptomatic and symptomatic individuals, and possibly the susceptible population into unvaccinated and vaccinated individuals. On the other hand, we extend the prophylactic opinion spectrum of Tyson et al. [22], introducing a prophylactic opinion field where attitudes/opinions toward both standard prophylactic measures (e.g. personal hygiene, face mask wearing and social distancing) and vaccination, and their interactions are integrated.

### *2.1. Disease dynamics*

We describe disease evolution using a compartmental model in which the target population is basically structured into Susceptible ($S$), Exposed ($E$), Infectious ($I$), Quarantined ($Q$), and Recovered individuals ($R$) [51–53]. But the infectious population is further distinguished into presymptomatic ($I_p$), asymptomatic ($I_a$), and symptomatic infectious ($I_s$) individuals, whereas the susceptible population ($S$) is distinguished into unvaccinated and completely susceptible individuals ($U$), and vaccinated and partially immunized individuals ($V$). The sizes of the susceptible and the infectious compartments satisfy respectively $S(t) = U(t) + V(t)$ and $I(t) = I_p(t) + I_a(t) + I_s(t)$ at time $t$, and the total population size $N(t)$ is given by

$$N(t) = U(t) + V(t) + E(t) + I_p(t) + I_a(t) + I_s(t) + Q(t) + R(t). \tag{1}$$

In a vaccination-free context (e.g. for a new emerging disease), the size of the vaccinated population is zero ($V(t) = 0$) and the susceptible population consists of only unvaccinated individuals ($S(t) = U(t)$). In this case, we have a SEIQR model, which is appropriate for

 doi:10.20944/preprints202212.0067.v1



the early phase of the COVID-19 pandemic. When vaccines become available, we have the more general UVEIQR model.

For simplicity, the susceptible population ($S$) is assumed homogeneous concerning factors such as age and medical conditions. We account for natural human demography, i.e. we include a natural death rate ($\mu$) for the whole population, and assume a constant timely number of new births and net immigration ($\eta$) entering the class $S$ of susceptibles (i.e. there is no immigration of infectives). Moreover, since the isolated infectious individuals do not mix actively with other classes, we assume that they do not have contacts sufficient for transmission with susceptible individuals [54–56]. Under the corresponding "quarantine-adjusted incidence" mechanism [57], the force of infection (i.e. the rate at which new infections ($E$) are produced) is given at time $t$ for a completely susceptible individual by

$$\lambda_o(t) = \frac{\beta_p I_p(t) + \beta_a I_a(t) + \beta_s I_s(t)}{N(t) - Q(t)}, \tag{2}$$

where $\beta_p$, $\beta_a$ and $\beta_s$ are baseline rates of contacts sufficient for transmission by presymptomatic, asymptomatic, and symptomatic infectious individuals, respectively. The available vaccines are considered imperfect, with an average efficacy of vaccine-induced protection $\kappa \in (0, 1)$. In other words, contacts between a $V$ individual and $I_p$, $I_a$ or $I_s$ individuals can be sufficient for transmission, but the force of infection is reduced to $(1 - \kappa)\lambda_o(t)$. A detailed description of both the SEIQR and the UVEIQR disease dynamics models in line with the known epidemiology of COVID-19 is given in Appendix A, along with graphical representations and mathematical descriptions based on nonlinear differential equations.

### *2.2. The Prophylactic Attitude Spectrum*

In a vaccination–free epidemic context, we follow Tyson et al. [22], assuming for simplicity that opinion dynamics only occur within the susceptible population $S$. The latter is distinguished into three groups of individuals that can be identified based on the level of prophylactic behaviour, which takes values in the prophylactic attitude spectrum:

$$\mathcal{P} = \{-1, 0, 1\}. \tag{3}$$

For any opinion $i \in \mathcal{P}$, $S_i$ denotes susceptibles with attitude $i$: $S_{-1}$ represents individuals with the highest prophylactic behaviour (and thus the least susceptible to the disease), and $S_1$ corresponds to individuals with the lowest prophylactic behaviour (and thus the most susceptible to the disease). Individuals $S_0$ in the middle of the spectrum correspond to an intermediate level of prophylactic behaviour. Note that if the opinion $i = -1$ is opposed to $i = 1$, then our model includes individuals with completely neutral position ($S_0$), unlike in the binary voter model based spectrum used by Tyson et al. [22]. However, the spectrum (3) simply defines the intensity of prophylactic behaviour on an ordinal scale, and high level attitude ($i = -1$) is not necessarily opposed to low level attitude ($i = 1$). The identity $S(t) = \sum_{i \in \mathcal{P}} S_i(t)$ holds for the susceptible population at time $t$.

### *2.3. The Source and Rate of Opinion Dynamics*

Opinion dynamics result from changes in opinions and behaviours over time, for instance, as the mass media diffuse information about disease prevalence or evolution of the pathogen or as disease surveillance and control policies are introduced or modified. Here, we adapt the "influence" approach of Tyson et al. [22], opinions being updated in response to interactions between susceptibles along the prophylactic opinion spectrum (3). In this framework, opinion dynamics within the susceptible population are governed by the rates (i.e. amplitudes) and the directions of mutual opinion influences.

The rate $\omega_i$ at which a susceptible individual $S_i$ influences the rest of the susceptible population is called the "influence function". For their SIR-Opinion dynamics model, Tyson

Preprints (www.preprints.org) | NOT PEER-REVIEWED | Posted: 5 December 2022 doi:10.20944/preprints202212.0067.v1



et al. [22] introduced linear and saturating influences as functions of the proportion of the infectious population ($I$). We consider here influence functions $\omega_i$ of the form

$$\omega_i(t) = w_i\Big(\widetilde{P}(t)\Big), \tag{4a}$$

where $w_i$ are Tyson et al. [22]'s fixed-order saturating extreme influence weights, and $\widetilde{P}(t)$ is the "perceived disease prevalence". The influence weights are given for $x \in [0,1]$ by

$$w_i(x) = \begin{cases} w_o\left[1 + w_\infty \frac{x}{(\tilde{k}+x)}\right] & \text{if} \quad i = -1 \\ w_o\left[1 + \frac{(w_\infty - 1)}{2} \frac{x}{(\tilde{k}+x)}\right] & \text{if} \quad i = 0 \\ w_o\left[1 - \frac{x}{(\tilde{k}+x)}\right] & \text{if} \quad i = 1 \end{cases}, \tag{4b}$$

with $w_o \in (0,1)$, the baseline influence rate for extreme opinions; $w_\infty \geq 1$, a skewness parameter; and $\tilde{k} > 0$, a half-saturation constant (see Appendix B for a graphical overview of $w_i$). In Equation(4a), we have substituted a perceived disease prevalence to the proportion of infectious ($I$) used by Tyson et al. [22], because, in our SEIQR model framework, the true disease prevalence given by $P(t) = [I_p(t) + I_a(t) + I_s(t) + Q(t)]/N(t)$ is unknown to any individual in the population (only $Q(t)$ is observable), and estimates of $P(t)$ reported by the mass media are perceived as disease prevalence. The perceived disease prevalence $\widetilde{P}$ is a determinant of opinion dynamics [58,59], and indeed, a source of changes in the rates of influences on and by prophylactic opinions, as implied by Equation(4a). Clearly, the under or over-estimation and reporting of disease prevalence by media or public health policymakers play a role in opinion dynamics.

Regarding the directions of influences, when an $S_i$ individual influences an $S_j$ individual, the $S_j$ individual changes his attitude by moving one step towards $i$ [22]. For instance, if the two individuals are at the opposite sides of the attitude spectrum (i.e. $i \times j < 0$), then the $S_j$ individual changes its attitude by moving one step towards the other side (i.e. $S_j \to S_0$). If, on the contrary, the interacting individuals have the same opinion (i.e. $i \times j > 0$), no change occurs. When an $S_i$ individual at a given side of the attitude spectrum ($i = \pm 1$) influences a moderate opinion holder $S_0$, then $S_0 \to S_i$. Finally, when an $S_j$ individual at a side of the spectrum ($j = \pm 1$) is influenced by an $S_0$ individual, then $S_j \to S_0$. These changes of opinions in the susceptible population can be summarized by the rates $\xi_{(i,j)}(t)$ of outgoing flows (opinion change $i \to j$) as:

$$\xi_{(-1,0)}(t) = \frac{\omega_0(t)S_0(t) + \omega_1(t)S_1(t)}{N(t) - Q(t)}, \tag{5a}$$

$$\xi_{(0,-1)}(t) = \frac{\omega_{-1}(t)S_{-1}(t)}{N(t) - Q(t)}, \tag{5b}$$

$$\xi_{(0,1)}(t) = \frac{\omega_1(t)S_1(t)}{N(t) - Q(t)}, \tag{5c}$$

$$\xi_{(1,0)}(t) = \frac{\omega_{-1}(t)S_{-1}(t) + \omega_0(t)S_0(t)}{N(t) - Q(t)}. \tag{5d}$$

### *2.4. The SEIQR-Opinion Dynamics Model*

The proposed SEIQR-Opinion dynamics model is depicted on the flow diagram in Figure 1. Note the use in Figure 1 of opinion-specific forces of infection ($\lambda_i$). Indeed, since increased levels of personal hygiene or social distancing from perceived sources of infection can substantively reduce both contacts and, if any, the sufficiency of contacts

Preprints (www.preprints.org) | NOT PEER-REVIEWED | Posted: 5 December 2022 doi:10.20944/preprints202212.0067.v1



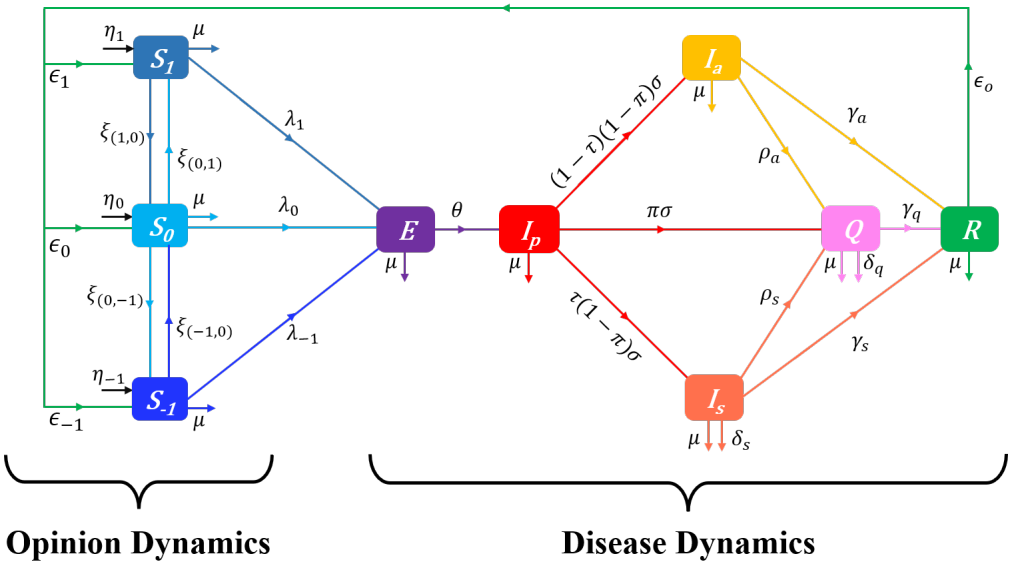


**Figure 1.** Flow-chart of a SEIQR-Opinion dynamics model showing the flow of humans between different compartments. The susceptible population is distinguished into individuals with the highest level of prophylactic behaviour ($S_{-1}$), individuals with the lowest level of prophylactic behaviour ($S_1$) and individuals with a middle level of prophylactic behaviour ($S_0$), $E$, $I_p$, $I_a$, $I_s$, $Q$ and $R$ denote the exposed, the presymptomatic infectious, the asymptomatic infectious, the symptomatic infectious, the quarantined, and the recovered populations, respectively. The parameters of the model are described in Table 1.

for transmission, we assume that an individual's attitude determines its susceptibility to infection in a way such that the force of infection for $S_i$ individuals has the form

$$\lambda_i(t) = \frac{\beta_{ip} I_p(t) + \beta_{ia} I_a(t) + \beta_{is} I_s(t)}{N(t) - Q(t)}, \tag{6a}$$

where, for $i \in \mathcal{P}$ and $j \in \{p, a, s\}$, $\beta_{ij}$ is the rate of contacts sufficient for transmission from an $I_j$ infectious to a $S_i$ susceptible. For simplicity, the dependence of infection rate on attitude is modeled using a single parameter [22]. It is specifically assumed that, for each infectious class $I_j$, the sufficient contact rate $\beta_{ij}$ is given by $\beta_{ij} = \varsigma_o^{1-i}\beta_j$, i.e.

$$\beta_{1j} = \beta_j, \quad \beta_{0j} = \varsigma_o \beta_j, \quad \beta_{-1j} = \varsigma_o^2 \beta_j, \tag{6b}$$

where $\beta_j$ is the baseline rate of sufficient contacts with $I_j$ infectious (this applies to $S_1$ susceptible individuals who have the lowest level of prophylactic behaviour), and $\varsigma_o \in (0, 1)$. From the structuring of the susceptible population $S$ in terms of prophylactic opinions $i$, the overall force of infection in the whole target population is given by the weighted average $\bar{\lambda}_o(t) = \frac{1}{S(t)} \sum_{i \in \mathcal{P}} S_i(t)\lambda_i(t)$. The SEIQR-Opinion dynamics model is described at time $t$ by the following system of nonlinear differential equations:

$$\dot{S}_{-1}(t) = \eta_{-1} + \xi_{(0,-1)}(t)S_0(t) - [\psi_{-1}(t) + \mu]S_{-1}(t) + \epsilon_{-1}R(t), \tag{7a}$$
$$\dot{S}_0(t) = \eta_0 + \xi_{(-1,0)}(t)S_{-1}(t) + \xi_{(1,0)}(t)S_1(t) - [\psi_0(t) + \mu]S_0(t) + \epsilon_0 R(t), \tag{7b}$$
$$\dot{S}_1(t) = \eta_1 + \xi_{(0,1)}(t)S_0(t) - [\psi_1(t) + \mu]S_1(t) + \epsilon_1 R(t), \tag{7c}$$
$$\dot{E}(t) = \lambda_{-1}(t)S_{-1}(t) + \lambda_0(t)S_0(t) + \lambda_1(t)S_1(t) - (\theta + \mu)E(t), \tag{7d}$$
$$\dot{I}_p(t) = \theta E(t) - (\sigma + \mu)I_p(t), \tag{7e}$$
$$\dot{I}_a(t) = (1-\tau)(1-\pi)\sigma I_p(t) - (\rho_a + \gamma_a + \mu)I_a(t), \tag{7f}$$
$$\dot{I}_s(t) = \tau(1-\pi)\sigma I_p(t) - (\rho_s + \gamma_s + \delta_s + \mu)I_s(t), \tag{7g}$$
$$\dot{Q}(t) = \pi\sigma I_p(t) + \rho_a I_a(t) + \rho_s I_s(t) - (\gamma_q + \delta_q + \mu)Q(t), \tag{7h}$$
$$\dot{R}(t) = \gamma_a I_a(t) + \gamma_s I_s(t) + \gamma_q Q(t) - (\epsilon_o + \mu)R(t), \tag{7i}$$

 doi:10.20944/preprints202212.0067.v1



with the nonnegative initial conditions $S_i(0) = S_{0i}$, $E(0) = E_0$, $I_p(0) = I_{0p}$, $I_a(0) = I_{0a}$, $I_s(0) = I_{0s}$, $Q(0) = Q_0$, and $R(0) = R_0$ where $(E_0, I_{0p}, I_{0a}, I_{0s}, Q_0, R_0)^\top \in [0, \infty)^6$, and $S_{0i} \geq 0$ for $i \in \mathcal{P}$. In System (7), the dots represent partial derivatives with respect to time $(t)$, $\psi_i$ denotes the time-dependent outgoing flows rate from $S_i$ susceptibles:

$$\psi_{-1}(t) = \xi_{(-1,0)}(t) + \lambda_{-1}(t), \tag{8a}$$

$$\psi_0(t) = \xi_{(0,-1)}(t) + \xi_{(0,1)}(t) + \lambda_0(t), \tag{8b}$$

$$\psi_1(t) = \xi_{(1,0)}(t) + \lambda_1(t), \tag{8c}$$

$\sum_{i \in \mathcal{P}} \eta_i = \eta$, $\sum_{i \in \mathcal{P}} \epsilon_i = \epsilon_o$, and the constant rate parameters of the model are described in Table 1. We shall use the qualifier "disease-dependent" for any solution for which there exists a finite time $t \geq 0$ such that $E(t) + I_p(t) + I_a(t) + I_s(t) > 0$.

Table 1: Description and values of parameters in the proposed models

| Parameter | Description | Values | Source |
|---|---|---|---|
| $\eta$ | Total recruitment rate (births and net immigration) | 35,615.35 | [54] |
| $\eta_u$ | Recruitment rate of non vaccinated individuals | $0.9999\eta$ | Assumed |
| $\eta_v$ | Recruitment rate of vaccinated individuals $(\eta - \eta_u)$ | $0.0001\eta$ | Assumed |
| $\eta_i$* | Recruitment rate of susceptibles with opinion $i$ | | |
| $\eta_{il}$* | Recruitment rate of susceptibles with opinions $i$ and $l$ | | |
| $\mu$ | Natural death rate | 0.00002 | [54] |
| $\beta_j$** | Baseline transmission rate by $I_j$ infectious $(j = p, a, s)$ | | |
| $\beta_{ij}$** | Transmission rate by $I_j$ infectious with opinion $i$ | | |
| $\varsigma_o$ | Prophylaxy-induced infection rate reduction factor | 0.5 | [22] |
| $\theta$ | Exit rate from incubation state (inverse of duration) | | |
| $\sigma$ | Exit rate from presymptomatic state | | |
| $\pi$ | Probability of early detection (presymptomatic stage) | | |
| $\tau$ | Proportion of symptomatic infectious | | |
| $\rho_j$** | Detection rate of $I_j$ infectious $(j = a, s)$ | | |
| $\gamma_j$** | Recovery rate of infectious $(j = a, s, q)$ | | |
| $\delta_j$** | Disease-related death rate of infectious $(j = s, q)$ | | |
| $\epsilon_o$ | Lost rate of disease-induced immunity | 0.011 | |
| $\epsilon_i$* | Part of recovered individuals with opinion $i$ | | |
| $\epsilon_{il}$* | Part of recovered individuals with opinions $i$ and $l$ | | |
| $\upsilon$ | Vaccination rate | 0.2 | Assumed |
| $\kappa$ | Average efficacy of available vaccines | 0.65 | Assumed |
| $\alpha$ | Lost rate of vaccine-induced immunity | 0.015 | Assumed |
| $w_o$ | Baseline influence rate (when disease is not perceived) | 0.1 | [22] |
| $w_\infty$ | Skewness parameter of influence functions | 2 | Assumed |
| $\tilde{k}$ | Half-influence saturation constant | 0.1 | [22] |

Table notes: All parameters take nonnegative values. The recruitment rates $\eta$, $\eta_u$, $\eta_v$, $\eta_i$, $\eta_{il}$ are in individuals per day, and all other rate parameters are in day$^{-1}$. *$i$ = level of prophylactic attitude defined in Equation (3), and $l = u$ (unfavorable to vaccines), $uv$ (favorable to vaccines, but unvaccinated), and $l = v$ (favorable to vaccines and vaccinated). **$j = p$ (presymptomatic), $a$ (asymptomatic), $s$ (symptomatic), or $q$ (quarantined) infectious.

### *2.5. The Prophylactic Attitude Field*

In addition to preventing infectious diseases through immunisation, vaccines have further benefits such as reduced antimicrobial resistance and herd protection for unvaccinated individuals, including the elderly with waning immune systems and those who are too young to be vaccinated or are immunosuppressed due to particular medical conditions [60,61]. Because these obvious advantages do not prevent controversies which feed vaccine-related opinion dynamics, especially in highly connected social networks [15–20], a disease–opinion dynamics model must account for the impact of vaccination on both attitudes and disease transmissions once vaccines are introduced into an epidemic context.

Although vaccination is also a prophylactic measure, the attitude toward vaccination may be inconsistent with other prophylactic behaviours. For instance, an individual with low

 doi:10.20944/preprints202212.0067.v1



prophylactic behaviour may get vaccinated to ignore social distancing. Likewise, an agent with an initially high prophylactic behaviour may become overconfident after vaccination and relax personal hygiene and social distancing, lowering its prophylactic behaviour [62]. Consequently, using one scale between two extreme opinions on prophylactic measures is not realistic in an epidemic context involving vaccination. Hence, we consider that the prophylactic opinion spectrum in Equation (3) excludes opinions on vaccination. A spectrum of vaccination-related opinions is separately introduced into the model, resulting in a bivariate field of opinions. For simplicity, we consider only two antagonists' opinions toward vaccines: favorable and unfavorable [11]. The bivariate attitude field is defined as

$$\mathcal{F} = \begin{Bmatrix} -1u, & 0u, & 1u \\ -1v, & 0v, & 1v \end{Bmatrix}, \tag{9}$$

where for each element $ij$, $i \in \mathcal{P}$ and $j \in \{u, v\}$, $j = u$ indexes individuals unfavorable to vaccination, and $j = v$ indexes individuals favorable to vaccination. In consequence, a class of $S_i$ susceptibles ($i \in \mathcal{P}$) is further structured into three groups: completely susceptible individuals unfavorable to vaccination ($U_{iu}$), completely susceptible individuals favorable to vaccination ($U_{iv}$), and susceptibles with active vaccine-induced immunity ($V_i$). The total susceptible population is then given by $S(t) = U(t) + V(t)$ where $U(t) = U_u(t) + U_v(t)$ denotes all completely susceptible individuals, $U_u(t) = \sum_{i\in\mathcal{P}} U_{iu}(t)$ denotes completely susceptible individuals unfavorable to vaccination, $U_v(t) = \sum_{i\in\mathcal{P}} S_{iv}(t)$ denotes completely susceptible individuals favorable to vaccination, and $V = \sum_{i\in\mathcal{P}} V_i(t)$ denotes vaccinated individuals. The identity $S(t) = \sum_{i\in\mathcal{P}} S_i(t)$ still holds for the whole susceptible population, and in addition, $S_i(t) = U_i(t) + V_i(t)$ where $U_i(t) = U_{iu}(t) + U_{iv}(t)$.

### *2.6. Changes in Prophylactic Attitudes in the Presence of Vaccination*

We still assume that opinion dynamics only occur within the susceptible population ($S$), including $U_u$, $U_v$ and $V$ individuals. Changes in opinion on prophylactic behaviours (excluding vaccination) are determined within $U_u$, $U_v$ or $V$ individuals by an "influence" process. Assuming for simplicity that the influence rates are *ceteris paribus* the same within the pro-vaccine and anti-vaccine susceptible populations as well as in the vaccinated population, the rates $\tilde{\xi}_{(i,j)}(t)$ of outgoing flows (opinion change $i \to j$) are defined by analogy to Equations (5a)–(5d) as:

$$\tilde{\xi}_{(-1,0)}(t) = \frac{\tilde{\omega}_0(t)S_0(t) + \tilde{\omega}_1(t)S_1(t)}{N(t) - Q(t)}, \tag{10a}$$

$$\tilde{\xi}_{(0,-1)}(t) = \frac{\tilde{\omega}_{-1}(t)S_{-1}(t)}{N(t) - Q(t)}, \tag{10b}$$

$$\tilde{\xi}_{(0,1)}(t) = \frac{\tilde{\omega}_1(t)S_1(t)}{N(t) - Q(t)}, \tag{10c}$$

$$\tilde{\xi}_{(1,0)}(t) = \frac{\tilde{\omega}_{-1}(t)S_{-1}(t) + \tilde{\omega}_0(t)S_0(t)}{N(t) - Q(t)}, \tag{10d}$$

where $\tilde{\omega}_i$ are influence functions. As the vaccination-free influence function $\omega_i$ defined in Equation (4a), the influence function $\tilde{\omega}_i$ depends on the perceived disease prevalence $\widetilde{P}$. However, in a vaccination-dependent epidemic context, the proportion of vaccinated individuals widely publicised in the mass media is also expected to impact prophylactic behaviours. It appears that when the influence of an individual with an opinion $i$ increases with $\widetilde{P}$, then it will likely decrease with the proportion of $V$ individuals (see e.g. [62]) and vice-versa. Assuming independence between the relative importance of $\widetilde{P}$ and $V$ in $\tilde{\omega}_i$, the influence rate is given the form

$$\tilde{\omega}_i(t) = w_o\frac{V(t)}{N(t)} + \left[1 - \frac{V(t)}{N(t)}\right] w_i\Big(\widetilde{P}(t)\Big) \tag{10e}$$

 doi:10.20944/preprints202212.0067.v1



so that $\tilde{\omega}_i(t) = \omega_i(t)$ if $V(t) = 0$, i.e. Equation (10e) is reduced to Equation (4a) in a vaccination-free context, and irrespective of the proportion $V(t)/N(t)$, $w_o$ remains the initial influence rate of an extreme opinion holder when the disease is not perceived ($\widetilde{P}(t) = 0$, i.e. an actual disease-free context, or a failure to detect any infectious individual although $I(t) > 0$). It is worth noting that the basic influence $w_i$ is a decreasing function for $i > 0$ and an increasing function for $i < 0$ (see graphics in Appendix B, see also Figure 1 in [22]). As a result, the influence $\tilde{\omega}_i$ of a high level prophylactic attitude ($i = -1$) increases with the perceived disease prevalence $\widetilde{P}(t)$ but decreases with the proportion $V(t)/N(t)$ of vaccinated individuals. Conversely, the influence of a low level prophylactic attitude ($i = 1$) decreases with $\widetilde{P}(t)$ but increases with $V(t)/N(t)$. It also stems from Equation (10e) that vaccination ($V(t) > 0$) reduces the slope of the influence rate for all prophylactic opinions. Specifically, when $x\%$ of the population is immunized through vaccination, the influences of prophylactic opinions become $(100 - x)\%$ less responsive to changes in the perceived disease prevalence $\widetilde{P}$, as compared to the response in a vaccination-free context.

### *2.7. Changes in Attitudes Towards Vaccination*

We consider that changes in opinion on vaccination among $U_i$ individuals ($U_{iu}$ and $U_{iv}$) are also governed by an "influence" process. Assuming that changes of attitude toward vaccines are independent of the level $i$ of prophylactic behaviour, the rate $\zeta_{(v,u)}(t)$ at which $U_{iv}$ individuals lose conviction to vaccination benefits and return to the class $U_{iu}$, and the rate $\zeta_{(u,v)}(t)$ at which $U_{iu}$ individuals become favourable to vaccines and enter the class $U_{iv}$ are given for any opinion $i \in \mathcal{P}$ by

$$\zeta_{(v,u)}(t) = \frac{\tilde{\omega}_u(t)U_u(t)}{N(t) - Q(t)}, \tag{11a}$$

$$\zeta_{(u,v)}(t) = \frac{\tilde{\omega}_v(t)[U_v(t) + V(t)]}{N(t) - Q(t)}, \tag{11b}$$

where $\tilde{\omega}_u$ and $\tilde{\omega}_v$ are influence functions related to opinions on vaccination. Note that individuals with vaccine-induced immunity ($V$) are all assumed to be favourable to vaccines (at least until the temporary immunity vanishes). To obtain simple expressions for the influence functions $\tilde{\omega}_u$ and $\tilde{\omega}_v$, we assume that there is no change in vaccine-related opinions when the disease is not perceived ($\widetilde{P}(t) = 0$), and the influence rates of pro-vaccine and anti-vaccine susceptibles are also constants when $V(t) = 0$, i.e. there is no shift in vaccine-related opinions until vaccination begins (note that this assumption is not as restrictive as it may first appear, because we have $V(t) > 0$ once trials for vaccine safety and efficacy start in the population, or even when only $\eta_v > 0$, i.e. vaccinated individuals only flow in from abroad). We also assume that an increase of either $\widetilde{P}(t)$ or $V(t)/N(t)$ leads to an increase in the influence of pro-vaccine susceptibles but a decrease in the influence of anti-vaccine susceptibles. These assumptions result in the influence functions:

$$\tilde{\omega}_u(t) = w_o\Big[1 - \widetilde{P}(t)\Big] + \widetilde{P}(t)w_1\left(\frac{V(t)}{N(t)}\right), \quad \text{and} \tag{11c}$$

$$\tilde{\omega}_v(t) = w_o\Big[1 - \widetilde{P}(t)\Big] + \widetilde{P}(t)w_{-1}\left(\frac{V(t)}{N(t)}\right). \tag{11d}$$

### *2.8. The UVEIQR-Opinion Dynamics Model*

We build a Disease-Opinion dynamics model by integrating prophylactic behaviours and vaccine-related opinions into the UVEIQR model. With the vaccination process, pro-vaccine susceptibles who have the prophylactic opinion $i$ ($U_{iv}$) get vaccinated (and enter the class $V_i$) at the same rate $\upsilon$ (irrespective of $i$). Likewise, the vaccinated individuals in $V_i$ lose their immunity and return to the class $U_{iv}$ at the rate $\alpha$. We also assume that anti-vaccine susceptibles ($U_u$) do not get vaccinated.

Preprints (www.preprints.org) | NOT PEER-REVIEWED | Posted: 5 December 2022 doi:10.20944/preprints202212.0067.v1



The opinion-specific force of infection $\lambda_i$ is given by Equation (6a) for $U_i$ individuals, and is $(1-\kappa)\lambda_i$ for $V_i$ individuals. The overall force of infection in the whole population is then given by the weighted average

$$\bar{\lambda}(t) = \frac{1}{S(t)} \sum_{i \in \mathcal{P}} [U_i(t) + (1-\kappa)V_i(t)]\lambda_i(t). \tag{12}$$

The flow diagram of the UVEIQR-Opinion dynamics model is shown in Figure 2. Let $\varphi_{il}$

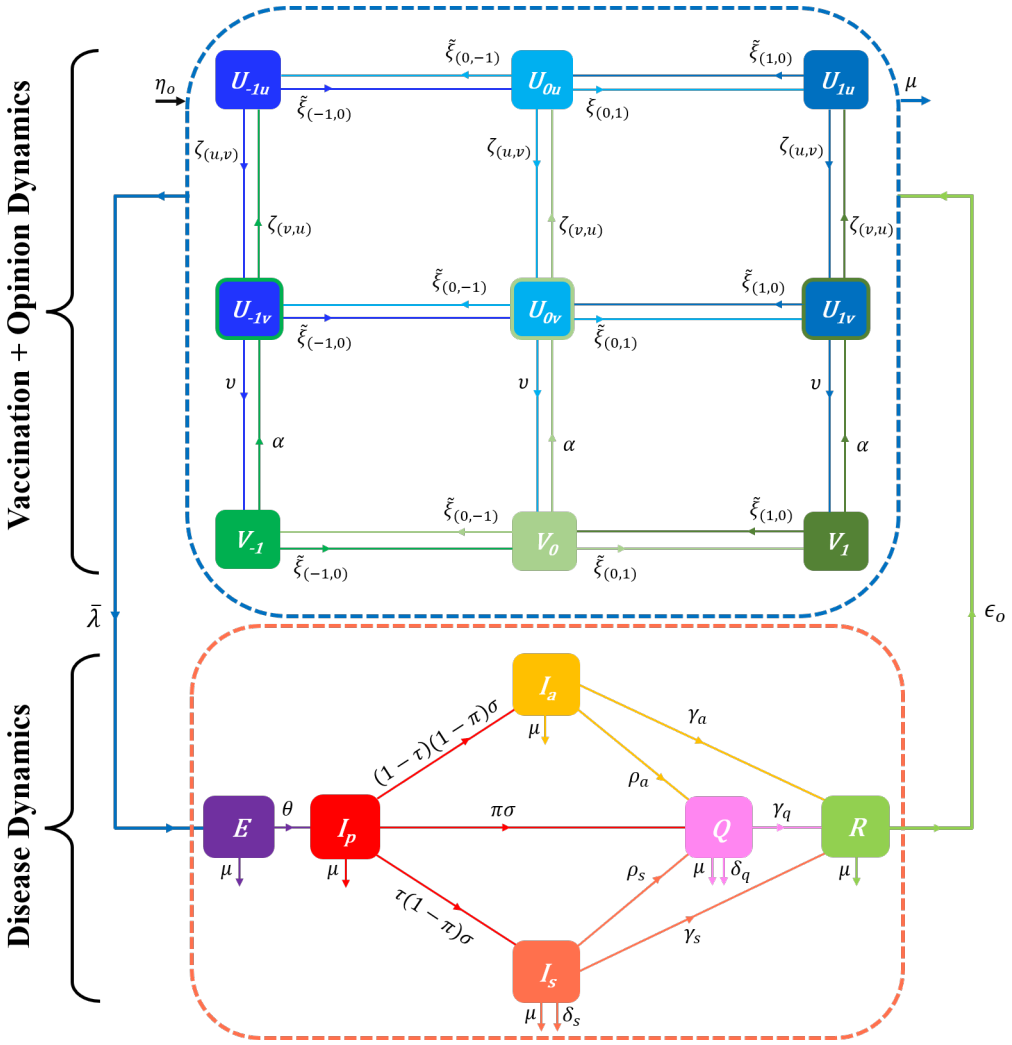


**Figure 2.** Flow-chart of a UVEIQR-Opinion dynamics model showing the flow of humans between different compartments. Susceptibles are distinguished into the unvaccinated (completely susceptible) population ($U$) and individuals with vaccine-induced partial immunity ($V$); the subscripts $u$ (unfavourable) and $v$ (favourable) indicate the attitude of $U$ individuals toward vaccination, the subscripts $i = -1, 0, 1$ indicate the level of prophylactic attitude ($i = -1$ is the highest level of prophylactic behaviour, $i = 1$ is the lowest level of prophylactic behaviour, and $i = 0$ is a middle level of prophylactic behaviour); $E$, $I_p$, $I_a$, $I_s$, $Q$ and $R$ denote respectively the exposed, the presymptomatic, the asymptomatic, and the symptomatic infectious, the quarantined, and the recovered populations. The parameters of the model are as described in Table 1.

denote for $l \in \{u, uv, v\}$ the opinion-related incoming flows for susceptible states:

$$\varphi_{-1u}(t) = \tilde{\xi}_{(0,-1)}(t)U_{0u}(t) + \zeta_{(v,u)}(t)U_{-1v}(t), \tag{13a}$$
$$\varphi_{0u}(t) = \tilde{\xi}_{(-1,0)}(t)U_{-1u}(t) + \tilde{\xi}_{(1,0)}(t)U_{1u}(t) + \zeta_{(v,u)}(t)U_{0v}(t), \tag{13b}$$
$$\varphi_{1u}(t) = \tilde{\xi}_{(0,1)}(t)U_{0u}(t) + \zeta_{(v,u)}(t)U_{1v}(t), \tag{13c}$$
$$\varphi_{-1uv}(t) = \tilde{\xi}_{(0,-1)}(t)U_{0v}(t) + \zeta_{(u,v)}(t)U_{-1u}(t) + \alpha V_{-1}(t), \tag{13d}$$
$$\varphi_{0uv}(t) = \tilde{\xi}_{(-1,0)}(t)U_{-1v}(t) + \tilde{\xi}_{(1,0)}(t)U_{1v}(t) + \zeta_{(u,v)}(t)U_{0u}(t) + \alpha V_0(t), \tag{13e}$$

Preprints (www.preprints.org) | NOT PEER-REVIEWED | Posted: 5 December 2022 doi:10.20944/preprints202212.0067.v1



$$\varphi_{1uv}(t) = \tilde{\xi}_{(0,1)}(t)U_{0v}(t) + \zeta_{(u,v)}(t)U_{1u}(t) + \alpha V_1(t), \tag{13f}$$
$$\varphi_{-1v}(t) = \tilde{\xi}_{(0,-1)}(t)V_0(t) + \upsilon U_{-1v}(t), \tag{13g}$$
$$\varphi_{0v}(t) = \tilde{\xi}_{(-1,0)}(t)V_{-1}(t) + \tilde{\xi}_{(1,0)}(t)V_1(t) + \upsilon U_{0v}(t), \tag{13h}$$
$$\varphi_{1v}(t) = \tilde{\xi}_{(0,1)}(t)V_{0v}(t) + \upsilon U_{1v}(t), \tag{13i}$$

and $\psi_{il}$ denote the time-dependent outgoing flow rates:

$$\psi_{-1u}(t) = \tilde{\xi}_{(-1,0)}(t) + \zeta_{(u,v)}(t) + \lambda_{-1}(t), \tag{13j}$$
$$\psi_{0u}(t) = \tilde{\xi}_{(0,-1)}(t) + \tilde{\xi}_{(0,1)}(t) + \zeta_{(u,v)}(t) + \lambda_0(t), \tag{13k}$$
$$\psi_{1u}(t) = \tilde{\xi}_{(1,0)}(t) + \zeta_{(u,v)}(t) + \lambda_1(t), \tag{13l}$$
$$\psi_{-1uv}(t) = \tilde{\xi}_{(-1,0)}(t) + \zeta_{(v,u)}(t) + \lambda_{-1}(t), \tag{13m}$$
$$\psi_{0uv}(t) = \tilde{\xi}_{(0,-1)}(t) + \tilde{\xi}_{(0,1)}(t) + \zeta_{(v,u)}(t) + \lambda_0(t), \tag{13n}$$
$$\psi_{1uv}(t) = \tilde{\xi}_{(1,0)}(t) + \zeta_{(v,u)}(t) + \lambda_1(t), \tag{13o}$$
$$\psi_{-1v}(t) = \tilde{\xi}_{(-1,0)}(t) + (1-\kappa)\lambda_{-1}(t), \tag{13p}$$
$$\psi_{0v}(t) = \tilde{\xi}_{(0,-1)}(t) + \tilde{\xi}_{(0,1)}(t) + (1-\kappa)\lambda_0(t), \tag{13q}$$
$$\psi_{1v}(t) = \tilde{\xi}_{(1,0)}(t) + (1-\kappa)\lambda_1(t). \tag{13r}$$

The proposed model is described at time $t$ by the following system of differential equations:

$$\dot{U}_{-1u}(t) = \eta_{-1u} + \varphi_{-1u}(t) - [\psi_{-1u}(t) + \mu]U_{-1u}(t) + \epsilon_{-1u}R(t), \tag{14a}$$
$$\dot{U}_{0u}(t) = \eta_{0u} + \varphi_{0u}(t) - [\psi_{0u}(t) + \mu]U_{0u}(t) + \epsilon_{0u}R(t), \tag{14b}$$
$$\dot{U}_{1u}(t) = \eta_{1u} + \varphi_{1u}(t) - [\psi_{1u}(t) + \mu]U_{1u}(t) + \epsilon_{1u}R(t), \tag{14c}$$
$$\dot{U}_{-1v}(t) = \eta_{-1uv} + \varphi_{-1uv}(t) - [\psi_{-1uv}(t) + \upsilon + \mu]U_{-1v}(t) + \epsilon_{-1uv}R(t), \tag{14d}$$
$$\dot{U}_{0v}(t) = \eta_{0uv} + \varphi_{0uv}(t) - [\psi_{0uv}(t) + \upsilon + \mu]U_{0v}(t) + \epsilon_{0uv}R(t), \tag{14e}$$
$$\dot{U}_{1v}(t) = \eta_{1uv} + \varphi_{1uv}(t) - [\psi_{1uv}(t) + \upsilon + \mu]U_{1v}(t) + \epsilon_{1uv}R(t), \tag{14f}$$
$$\dot{V}_{-1}(t) = \eta_{-1v} + \varphi_{-1v}(t) - [\psi_{-1v}(t) + \alpha + \mu]V_{-1}(t), \tag{14g}$$
$$\dot{V}_0(t) = \eta_{0v} + \varphi_{0v}(t) - [\psi_{0v}(t) + \alpha + \mu]V_0(t), \tag{14h}$$
$$\dot{V}_1(t) = \eta_{1v} + \varphi_{1v}(t) - [\psi_{1v}(t) + \alpha + \mu]V_1(t), \tag{14i}$$
$$\dot{E}(t) = \bar{\lambda}(t)S(t) - (\theta + \mu)E(t), \tag{14j}$$
$$\dot{I}_p(t) = \theta E(t) - (\sigma + \mu)I_p(t), \tag{14k}$$
$$\dot{I}_a(t) = (1-\tau)(1-\pi)\sigma I_a(t) - (\rho_a + \gamma_a + \mu)I_a(t), \tag{14l}$$
$$\dot{I}_s(t) = \tau(1-\pi)\sigma I_p(t) - (\rho_s + \gamma_s + \delta_s + \mu)I_s(t), \tag{14m}$$
$$\dot{Q}(t) = \pi\sigma I_p(t) + \rho_a I_a(t) + \rho_s I_s(t) - (\gamma_q + \delta_q + \mu)Q(t), \tag{14n}$$
$$\dot{R}(t) = \gamma_a I_a(t) + \gamma_s I_s(t) + \gamma_q Q(t) - (\epsilon_o + \mu)R(t), \tag{14o}$$

with the nonnegative initial conditions $U_{il}(0) = U_{0il}$, $V_i(0) = V_{0i}$, $E(0) = E_0$, $I_p(0) = I_{0p}$, $I_a(0) = I_{0a}$, $I_s(0) = I_{0s}$, $Q(0) = Q_0$, and $R(0) = R_0$ where $U_{0il} \geq 0$ and $V_{0i} \geq 0$ for $i \in \mathcal{P}$ and $l \in \{u, uv, v\}$, and $(E_0, I_{0p}, I_{0a}, I_{0s}, Q_0, R_0)^\top \in [0,\infty)^6$. In Equations (14a)–(14o), $\sum_{i\in\mathcal{P}}\sum_{l=u,uv,v}\eta_{il} = \eta$, $\sum_{i\in\mathcal{P}}\sum_{l=u,uv}\epsilon_{il} = \epsilon_o$ (e.g. $\epsilon_{il} = \epsilon_o/6$ for an equal repartition; or $\epsilon_{0l} = \epsilon_o/4$ and $\epsilon_{-1l} = \epsilon_{1l} = \epsilon_o/8$ assuming that 50% of recovered individuals have a moderate prophylactic attitude), and the constant rate parameters of the model are described in Table 1.

Note that in the special case $\upsilon = 0$ and $V_{0i} = \eta_{iv} = 0$ for $i \in \mathcal{P}$, model (14) is reduced to the vaccination-free model (7) where $S_i$ susceptibles are divided into $U_{iu}$ and $U_{iv}$ with constant mutual influence rates $\tilde{\omega}_u(t) = \tilde{\omega}_v(t) = w_o$ (but with no incidence on disease dynamics or basic prophylactic opinion dynamics).

 doi:10.20944/preprints202212.0067.v1



## 3. Analytical Results

The first important property of any mathematical model for a biological process is, of course, biological meaningfulness. The following result guarantees that the UVEIQR-Opinion model always has a biological interpretation.

**Lemma 1** (Non-negativity and Boundedness)**.** *Under the nonnegative initial conditions* $U_{iu}(0) \geq 0$, $U_{iv}(0) \geq 0$, $V_i(0) \geq 0$ *for* $i \in \mathcal{P}$, $E(0) \geq 0$, $I_p(0) \geq 0$, $I_a(0) \geq 0$, $I_s(0) \geq 0$, $Q(0) \geq 0$ *and* $R(0) \geq 0$, *all solutions of Systems* (14) *remain nonnegative and are bounded at any time* $t > 0$. *The total population size* $N(t)$ *is in particular bounded as* $0 \leq N(t) \leq \widehat{N}$ *where* $\widehat{N} = \max\{N(0), N^c\}$ *with* $N^c = \eta/\mu$ *the carrying capacity in disease–free conditions.*

Since System (7) is a special case of System (14), Lemma 1 also assures that all solutions of the SEIQR-Opinion model (7) are biologically meaningful. In the remainder of this section, we present some important properties of disease-opinion dynamics in a population described by the introduced models. The similar mathematical properties of the models with no differential opinion are given in Appendix A.3, and the proofs of all results are given in Appendix C. Unlike in Lemma 1, we start for clarity with the properties of the simpler model (7) without vaccination ($\upsilon = 0$ and $V_{0i} = \eta_{iv} = 0$ for $i \in \mathcal{P}$) and then discuss the changes induced by the introduction of vaccines in both disease and opinion dynamics in the model (14).

### *3.1. Vaccination–free Disease–free Equilibrium and Reproduction Numbers*

To summarize the dynamics of a population described by the SEIQR-Opinion model (7), we find the disease-free equilibrium (DFE) of the model and use it to obtain the effective reproduction number by the next-generation matrix approach [63]. We further derive critical detection rates to achieve disease eradication in the long-run.

**Proposition 1** (Vaccination–free DFE & Reproduction Number)**.** *The SEIQR-Opinion model* (7) *has a unique DFE given for* $w_o > 0$ *by*

$$\boldsymbol{X}^c = (S^c_{-1}, S^c_0, S^c_1, 0, 0, 0, 0, 0, 0)^\top \quad \text{where} \tag{15a}$$

$$S^c_{-1} = \frac{\eta_{-1}}{\mu} - \frac{1}{2}\left(S^c_0 - \frac{\eta_0}{\mu}\right), \tag{15b}$$

$$S^c_0 = \eta\left(\frac{1}{\mu} + \frac{1}{w_o}\right) - \sqrt{\frac{4\eta\eta_1}{\mu w_o} + \left(\frac{\eta_1 - \eta_{-1}}{\mu} - \frac{\eta}{w_o}\right)^2}, \tag{15c}$$

$$S^c_1 = \frac{\eta_1}{\mu} - \frac{1}{2}\left(S^c_0 - \frac{\eta_0}{\mu}\right). \tag{15d}$$

*When* $w_o = 0$, *we have* $S^c_i = \frac{\eta_i}{\mu}$ *for* $i \in \mathcal{P}$. *Moreover, for a population described by System* (7), *the basic reproduction number is given by*

$$\mathcal{R}_0(\pi, \rho_a, \rho_s, w_o) = \sum_{i\in\mathcal{P}} \sum_{j=p,a,s} \mathcal{R}_{0ij} \qquad \text{where} \tag{16a}$$

$$\mathcal{R}_{0ij} = \frac{\theta}{(\theta+\mu)(\sigma+\mu)} \frac{S^c_i \varsigma_o^{1-i}}{N^c} \beta_j m_j$$

*is the contribution of* $S_i$ *susceptibles and* $I_j$ *infectious to* $\mathcal{R}_0$, *with* $m_p = 1$, $m_a = \frac{(1-\tau)(1-\pi)\sigma}{\rho_a+\gamma_a+\mu}$, *and* $m_s = \frac{\tau(1-\pi)\sigma}{\rho_s+\gamma_s+\delta_s+\mu}$. *Furthermore, the basic reproduction number* $\mathcal{R}_0$ *decreases with the baseline influence rate* $w_o$ *(provided that the prophylaxis-induced infection rate reduction factor* $\varsigma_o$ *satisfies* $\varsigma_o < 1$*). The time-varying effective reproduction number is given by*

$$\mathcal{R}_t = \frac{\theta}{(\theta+\mu)(\sigma+\mu)} \sum_{i\in\mathcal{P}} \frac{S_i(t)\varsigma_o^{1-i}}{N(t) - Q(t)} \sum_{j=p,a,s} \beta_j m_j. \tag{16b}$$

Preprints (www.preprints.org) | NOT PEER-REVIEWED | Posted: 5 December 2022 doi:10.20944/preprints202212.0067.v1



**Remark 1.** *In the absence of opinion dynamics ($w_o = 0$), each class of susceptibles $S_i$ approaches its carrying capacity $\frac{\eta_i}{\mu}$.*

**Remark 2.** *The stationary sizes of $S_{-1}$ and $S_1$ susceptibles decrease with the baseline influence rate $w_o$ whereas $S_0$ increases with $w_o$. Indeed, the mutual influences of $S_0$ and $S_i$ individuals ($i = \pm 1$) balance and cancel each other, whereas interactions between individuals on the opposite sides of the attitude spectrum lead to positive flows into $S_0$. As a result, if the recruitment rates are equal across susceptible states ($\eta_i = \eta/3$), then more than a third of the long-run population will have a moderate prophylactic attitude in the absence of disease. The decay of the basic reproduction number $\mathcal{R}_0$ as a function of the baseline influence rate $w_o$ is another consequence of this stationary dynamics.*

**Remark 3.** *The basic reproduction number $\mathcal{R}_0$ accounts for the implementation of a disease surveillance mechanism, if any (i.e. the detection rates $\pi$, $\rho_a$ and $\rho_s$ can be positive even in a disease-free context). In an emerging disease context (e.g. right before the report in late December 2020 of the first confirmed COVID-19 case), some symptoms might be unknown, and test kits might not be yet developed or available. In the special case where $\pi \approx \rho_a \approx \rho_s \approx 0$, the basic reproduction number is*

$$\mathcal{R}_o = \frac{\theta}{(\theta+\mu)(\sigma+\mu)}\left[\beta_p + \frac{(1-\tau)\sigma}{\gamma_a+\mu}\beta_a + \frac{\tau\sigma}{\gamma_s+\delta_s+\mu}\beta_s\right]\frac{\mu}{\eta}\sum_{i\in\mathcal{P}} S_i^c \varsigma_o^{1-i} \tag{17}$$

*which satisfies $\mathcal{R}_o \geq \mathcal{R}_0(\pi, \rho_a, \rho_s, w_o) \geq \mathcal{R}_0(1, \rho_a, \rho_s, w_o)$* ceteris paribus.

The first measures implemented after the epidemic outbreak of a contagious disease is the identification and isolation of infectious individuals. The detection/isolation effort (targeting and testing of most susceptible groups, contact tracing, voluntary mass testing campaign, systematic testing) is critical to the control of the propagation of the disease in the absence of vaccination. Such measures can sufficiently contain an epidemic under some conditions detailed in the following corollary of Proposition 1.

**Corollary 1** (Critical Detection Rates)**.** *Suppose that $\mathcal{R}_0(1, \rho_a, \rho_s, w_o) < 1$.*

*If $\mathcal{R}_0(0, \rho_a, \rho_s, w_o) > 1$, then the critical (minimal) early detection probability required to sufficiently lower $\mathcal{R}_0$ and ensure disease eradication in the long run is*

$$\pi^*(\rho_a, \rho_s, w_o) = 1 - \frac{\frac{(\theta+\mu)(\sigma+\mu)\eta}{\theta\mu\left(\sum_{i\in\mathcal{P}} S_i^c \varsigma_o^{1-i}\right)} - \beta_p}{\sigma\left[\frac{(1-\tau)\beta_a}{\rho_a+\gamma_a+\mu} + \frac{\tau\beta_s}{\rho_s+\gamma_s+\delta_s+\mu}\right]} \tag{18a}$$

*which decreases with the baseline influence rate $w_o$, and the detection rates $\rho_a$ of asymptomatic infectious and $\rho_s$ of symptomatic infectious. If $\mathcal{R}_0(\pi, 1, \rho_s, w_o) < 1 < \mathcal{R}_0(\pi, 0, \rho_s, w_o)$, then the critical (minimal) detection rate of asymptomatic infectious is*

$$\rho_a^*(\pi, \rho_s, w_o) = \left[\frac{(1-\pi)(1-\tau)\sigma\beta_a}{\frac{(\theta+\mu)(\sigma+\mu)\eta}{\theta\mu\left(\sum_{i\in\mathcal{P}} S_i^c \varsigma_o^{1-i}\right)} - \beta_p - \frac{(1-\pi)\tau\sigma\beta_s}{\rho_s+\gamma_s+\delta_s+\mu}}\right] - \gamma_a - \mu \tag{18b}$$

*which decreases with $\pi$, $\rho_s$, and $w_o$. Likewise, if $\mathcal{R}_0(\pi, \rho_a, 1, w_o) < 1 < \mathcal{R}_0(\pi, \rho_a, 0, w_o)$, then the critical (minimal) detection rate of asymptomatic infectious is*

$$\rho_s^*(\pi, \rho_s, w_o) = \left[\frac{(1-\pi)\tau\sigma\beta_s}{\frac{(\theta+\mu)(\sigma+\mu)\eta}{\theta\mu\left(\sum_{i\in\mathcal{P}} S_i^c \varsigma_o^{1-i}\right)} - \beta_p - \frac{(1-\pi)(1-\tau)\sigma\beta_a}{\rho_a+\gamma_a+\mu}}\right] - \gamma_s - \delta_s - \mu \tag{18c}$$

*which decreases with $\pi$, $\rho_a$, and $w_o$.*

 doi:10.20944/preprints202212.0067.v1



It appears that if $\mathcal{R}_0 < 1$ in a hypothetical scenario where all infectious individuals are isolated at the presymptomatic stage, then mass testing and quarantining can be sufficient to ensure that an epidemic is unsustainable in the target population. If $\mathcal{R}_0(1, \rho_a, \rho_s, w_o) > 1$, then it is not possible to contain the epidemic of the target contagious disease using isolation measures only. It remains, however, likely to break the transmission dynamics by reducing exposition to the disease, i.e. the rate of sufficient contact between potentially infectious and susceptible individuals (for COVID-19, this included, e.g. social distancing, face mask wearing, school closing, curfew, ban of gatherings, lockdown). The introduction of vaccination is the ultimate solution to reduce transmissions while alleviating the social and economic drawbacks of the first containment measures.

### *3.2. Disease–free Equilibrium and Reproduction Numbers in a Vaccination Context*

We find the disease-free equilibrium for a population described by the UVEIQR-Opinion model (14), and compute the related control reproduction number. We further discuss the critical vaccination rate to ensure disease eradication in the long-run.

**Proposition 2** (Disease–free Equilibrium & Reproduction Number)**.** *The UVEIQR-Opinion model (14) admits a unique disease-free equilibrium given for $w_o > 0$ by*

$$\boldsymbol{X}^c = \left((\boldsymbol{S}^c)^\top, 0, 0, 0, 0, 0\right)^\top, \tag{19a}$$

*where $\boldsymbol{S}^c = \left(U^c_{-1u}, U^c_{0u}, U^c_{1u}, U^c_{-1v}, U^c_{0v}, U^c_{1v}, V^c_{-1}, V^c_0, V^c_1\right)^\top$ is given by*

$$\boldsymbol{S}^c = \boldsymbol{M}^{-1}\boldsymbol{\eta} \quad \text{with} \tag{19b}$$

$$\boldsymbol{\eta} = (\eta_{-1u}, \eta_{0u}, \eta_{1u}, \eta_{-1uv}, \eta_{0uv}, \eta_{1uv}, \eta_{-1v}, \eta_{0v}, \eta_{1v})^\top,$$

$$\boldsymbol{M} = \frac{w_o}{N^c}\begin{pmatrix} \boldsymbol{M}_u & -U^c_u\boldsymbol{I}_3 & \boldsymbol{0} \\ -(U^c_v + V^c)\boldsymbol{I}_3 & \boldsymbol{M}_{uv} & -\frac{N^c}{w_o}\alpha\boldsymbol{I}_3 \\ \boldsymbol{0} & -\frac{N^c}{w_o}\upsilon\boldsymbol{I}_3 & \boldsymbol{M}_v \end{pmatrix} + \mu\boldsymbol{I}_9, \tag{19c}$$

$$U^c_u = \frac{\eta\eta_{uu}(\alpha+\mu)}{w_o\mu(\eta_v + \upsilon U^c_v) + \eta\mu(\alpha+\mu)}, \tag{19d}$$

$$U^c_v = \begin{cases} \frac{w_o C}{(\alpha+\mu)\eta + w_o\eta_v} & \text{if} \quad \upsilon = 0 \\ \\ \frac{\sqrt{B^2+4AC}-B}{2A} & \text{if} \quad \upsilon \neq 0 \end{cases}, \tag{19e}$$

$$V^c = \frac{\eta_v + \upsilon U^c_v}{\alpha+\mu}, \tag{19f}$$

$$\boldsymbol{M}_u = \boldsymbol{M}_0 + (U^c_v + V^c)\boldsymbol{I}_3,$$

$$\boldsymbol{M}_{uv} = \boldsymbol{M}_0 + \left(U^c_u + \frac{N^c}{w_o}\upsilon\right)\boldsymbol{I}_3,$$

$$\boldsymbol{M}_v = \boldsymbol{M}_0 + \frac{N^c}{w_o}\alpha\boldsymbol{I}_3,$$

$$\boldsymbol{M}_0 = \begin{pmatrix} S^c_0 + S^c_1 & -S^c_{-1} & 0 \\ -(S^c_0 + S^c_1) & S^c_{-1} + S^c_1 & -(S^c_{-1} + S^c_0) \\ 0 & -S^c_1 & S^c_{-1} + S^c_0 \end{pmatrix},$$

*where we have set $A = \upsilon\left(1 + \frac{\upsilon}{\alpha+\mu}\right)$, $B = \eta_u\left(\frac{\alpha+\upsilon+\mu}{w_o} - \frac{\upsilon}{\mu}\right) + \eta_v\left(1 + \frac{\alpha+\upsilon+\mu}{w_o} + \frac{\upsilon(\mu-\alpha)}{\mu(\alpha+\mu)}\right)$ and $C = \eta\eta_{uv}\frac{\alpha+\mu}{w_o\mu} + \frac{\eta_v}{\mu}\left(\eta_u + \frac{\alpha}{\alpha+\mu}\eta_v + \frac{\alpha}{w_o}\eta\right)$, $\eta_{uu} = \sum_{i\ \in\mathcal{P}}\eta_{iu}$, $\eta_u = \sum_{i\ \in\mathcal{P}}(\eta_{iu} + \eta_{iuv})$, $\eta_v = \sum_{i\ \in\mathcal{P}}\eta_{iv}$, and $\boldsymbol{I}_n$ denotes the $n \times n$ identity matrix. In the absence of opinion*

*dynamics ($w_o = 0$), we have $U_{iu}^c = \frac{\eta_{iu}}{\mu}$, $U_{iv}^c = \frac{\eta_{iuv}}{\mu}$, and $V_i^c = \frac{\eta_{iv}}{\mu}$ for $i \in \mathcal{P}$. Moreover, for a population described by System (14), the control reproduction number is given by*

$$\mathcal{R}_c(\upsilon, \kappa, \alpha, w_o) = \sum_{i\in\mathcal{P}} \sum_{j=p,a,s} \mathcal{R}_{cij} \qquad \text{where} \tag{20a}$$

$$\mathcal{R}_{cij} = \frac{\theta}{(\theta+\mu)(\sigma+\mu)} \frac{[U_i^c + (1-\kappa)V_i^c]\varsigma_o^{1-i}}{N^c} \beta_j m_j$$

*is the contribution of $S_i$ susceptibles and $I_j$ infectious to $\mathcal{R}_c$, with $U_i^c = U_{iu}^c + U_{iv}^c$. The control reproduction number $\mathcal{R}_c$ decreases with the vaccination rate $\upsilon$ and the baseline influence rate $w_o$, and satisfies*

$$(1-\kappa)\mathcal{R}_0 \leq \mathcal{R}_c(\upsilon, \kappa, \alpha, w_o) \leq \mathcal{R}_0. \tag{20b}$$

*The time-varying effective reproduction number is given by*

$$\mathcal{R}_{ct}(\upsilon, \kappa, \alpha, w_o) = \sum_{i\in\mathcal{P}} \sum_{j=p,a,s} \mathcal{R}_{cijt} \qquad \text{where} \tag{20c}$$

$$\mathcal{R}_{cijt} = \frac{\theta}{(\theta+\mu)(\sigma+\mu)} \frac{[U_i(t) + (1-\kappa)V_i(t)]\varsigma_o^{1-i}}{N(t) - Q(t)} \beta_j m_j.$$

**Remark 4.** *The expression of $\boldsymbol{S}^c$ in matrix notation given by Equation (19b) is developed in Appendix D where a formula is provided for each of the nine elements of $\boldsymbol{S}^c$.*

It appears from Equation (20a) that, as expected, $\mathcal{R}_c$ decreases with both vaccination rate ($\upsilon$) and average vaccine efficacy ($\kappa$) but increases with the immunity lost rate ($\alpha$). Inequality (20b) recognizes that vaccine efficacy is an important parameter in disease control: $\mathcal{R}_c$ cannot fall under $(1-\kappa)\mathcal{R}_0$ even for a large vaccination rate $\upsilon$. On setting

$$\kappa^* = \frac{\mathcal{R}_0 - 1}{\mathcal{R}_0} \tag{21}$$

for $\mathcal{R}_0 > 1$, a necessary condition for disease eradication is that the average vaccine efficacy must satisfy $\kappa > \kappa^*$ (ensuring $(1-\kappa)\mathcal{R}_0 < 1$). The following corollary gives the critical vaccination rate to eradicate the disease for a fixed average vaccine efficacy $\kappa$.

**Corollary 2** (Critical Vaccination Rate)**.** *If $\mathcal{R}_0 > 1$ and $\kappa > \kappa^*$, then the critical (minimal) vaccination rate required to sufficiently lower $\mathcal{R}_c$ and ensure disease eradication in the long-run is*

$$\upsilon^*(\kappa, \alpha) = \frac{(\alpha+\mu)(\mathcal{R}_0 - 1) - \kappa p_v \mu \mathcal{R}_0}{1 - (1-\kappa)\mathcal{R}_0} \tag{22a}$$

*which increases with the immunity lost rate $\alpha$ decreases with $\kappa$ and satisfies*

$$\upsilon^* > (\alpha+\mu)(\mathcal{R}_0 - 1) - p_v \mu \mathcal{R}_0. \tag{22b}$$

### *3.3. Persistence of the Disease*

If $\mathcal{R}_c > 1$, then any introduction of infectious individuals has the potential to kick off and maintain an epidemic outbreak, as per the next proposition.

**Proposition 3** (Persistence of the Disease)**.** *For the UVEIQR-Opinion model (14). If $\mathcal{R}_c > 1$, then the disease persists uniformly, i.e. there exists a positive real constant $\varrho$ independent of the initial data, such that for any disease-dependent solution $\boldsymbol{X} = (U_{-1u}, U_{0u}, U_{1u}, U_{-1v}, U_{0v}, U_{1v}, V_{-1}, V_0, V_1, E, I_p, I_a, I_s, Q, R)^\top$, we have:*

$$\lim_{t\to\infty} x(t) \geq \varrho \quad \text{for} \quad x \in \{U_{-1u}, U_{0u}, U_{1u}, U_{-1v}, U_{0v}, U_{1v}, E, I_p, I_a, I_s, Q, R\}, \tag{23a}$$

Preprints (www.preprints.org) | NOT PEER-REVIEWED | Posted: 5 December 2022 doi:10.20944/preprints202212.0067.v1



$$\lim_{t\to\infty} V_i(t) \geq \varrho \quad \text{when} \quad \eta_v > 0 \quad \text{or} \quad \upsilon > 0, \quad \text{and} \tag{23b}$$

$$\lim_{t\to\infty} V_i(t) = 0 \quad \text{when} \quad \eta_v = \upsilon = 0. \tag{23c}$$

## 4. Limits and Perspectives

Because of the relatively large number of possible states in the models introduced for disease-opinion dynamics, some simple assumptions were made in the model construction to reduce the number of model parameters on the one hand and primarily to obtain a minimum of analytical closed form results on the other hand. Ahead is the use of a unique class of exposed individuals, irrespective of the vaccination status of the individuals before the exposition. Although this assumption may hold for some diseases, it is not realistic in the ongoing COVID-19 pandemic context since the effects of the currently available COVID-19 vaccines are beyond a mere reduction in the force of infection. Indeed, the vaccines also reduce the risk of severe forms of the disease (requiring respiratory assistance), transmission from vaccinated infected, risk of long-term sequels, and disease-related mortality [64,65] so that the paths from exposition to recovery should be different for vaccinated individuals as compared to non-vaccinated individuals. In addition, no age structure is included in the proposed models, although COVID-19 transmission and mortality rates and vaccination scenarios are highly age-dependent [66–69]. Another source of complexity we did not account for is the co-existence of many variants of SARS-CoV-2 with different transmission and mortality rates in a target human population [70,71].

Many strong assumptions were also made regarding opinion dynamics. The strongest one is likely that opinion dynamics only occur in the susceptible population. As in Tyson et al. [22], this assumption greatly simplifies model equations. Though, all individuals in disease-dependent states, including the non-mixing population $Q$ (which can interact with susceptibles by, e.g. phone, social media, ...), can obviously influence the opinions of susceptibles. For instance, the prophylactic opinions of physically isolated ($Q$) and recovered ($R$) individuals can change in response to being aware of their current or past infectious state. These opinion dynamics can then contribute to the overall influence of a given opinion $i$ holders on susceptibles with a different opinion $j \neq i$. Clearly, as for susceptibles, disease-dependent classes should also be differentiated according to opinions, and their interactions with other classes allowed to influence, to some extent, the attitude of susceptible individuals. Another strong assumption is considering only one prophylactic attitude level for each prophylactic opinion. This hypothesis supposes that all individuals with a given opinion have the same prophylactic attitude level (same degree of opinion) and thereby hides interactions between like-minded individuals. Consequently, the assumption neglects amplification of opinion, a phenomenon which can substantially impact opinion dynamics [22].

Another important assumption is that all individuals have the same baseline influence rate $w_o$ in disease-free conditions, irrespective of prophylactic opinion. Instead of Equation (4b), the basic influence weights $w_i$ can have, for $x \in [0,1]$, the more general form

$$w_i(x) = \begin{cases} w_o\left[1 + w_\infty \frac{x}{(\tilde{k}+x)}\right] & \text{if} \quad i = -1 \\ w_o\left[\phi + \frac{(w_\infty - \phi)}{2}\frac{x}{(\tilde{k}+x)}\right] & \text{if} \quad i = 0 \\ w_o\left[1 - \frac{x}{(\tilde{k}+x)}\right] & \text{if} \quad i = 1, \end{cases} \tag{24a}$$

where $\phi \in (0,1]$ is a baseline influence rate reduction factor for a moderate opinion. In Equation (24a), the parameter $\phi$ allows to reduce the influence rate of moderate prophylactic opinion holders ($i = 0$) relative to extreme opinion holders ($i = \pm 1$). The model presented in Section 2 corresponds to the special case $\phi = 1$. In this modified influence process based

Preprints (www.preprints.org) | NOT PEER-REVIEWED | Posted: 5 December 2022 doi:10.20944/preprints202212.0067.v1



on Equations (24a) and (24b), Equation (10e) defining influence rates in a vaccination-dependent context becomes

$$\tilde{\omega}_i(t) = w_o \phi^{1-|i|} \frac{V(t)}{N(t)} + \left[1 - \frac{V(t)}{N(t)}\right] w_i\Big(\widetilde{P}(t)\Big). \tag{24b}$$

The resulting extended SEIQR-Opinion model admits, for $w_o > 0$ and $\phi < 1$, disease-free equilibriums of the form $\boldsymbol{X}^c = \left(S^c_{-1}, S^c_0, S^c_1, 0, 0, 0, 0, 0, 0\right)^\top$ where

$$S^c_{-1} = \frac{\eta_{-1}}{\mu} - \frac{1}{2}\left[N^c + \frac{\eta}{w_o} - \sqrt{\Delta} - (1-\phi)S^c_0\left[1 + \frac{w_o(\eta_1 - \eta_{-1})}{\mu[\eta - w_o(1-\phi)S^c_0]}\right] - \frac{\eta_0}{\mu}\right], \tag{25a}$$

$$S^c_0 = \frac{1}{1-\phi}\left[\frac{\eta}{w_o} - \text{Proot}(\boldsymbol{a})\right], \tag{25b}$$

$$S^c_1 = \frac{\eta_1}{\mu} - \frac{1}{2}\left[N^c + \frac{\eta}{w_o} - \sqrt{\Delta} - (1-\phi)S^c_0\left[1 - \frac{w_o(\eta_1 - \eta_{-1})}{\mu[\eta - w_o(1-\phi)S^c_0]}\right] - \frac{\eta_0}{\mu}\right], \tag{25c}$$

where $\Delta = 2N^c\left(\frac{\eta_{-1}+\eta_1}{w_o}\right) + \left[\frac{\eta}{w_o} - (1-\phi)S^c_0\right]^2 + \left[\frac{\eta_{-1}-\eta_1}{\mu-(1-\phi)w_o S^c_0/N^c}\right]^2$, $\text{Proot}(\cdot)$ returns the positive roots of the polynomial defined for $x$ as $\sum_{k=1}^{5} a_k x^{k-1}$, with $a_k$ the $k$th element of the vector $\boldsymbol{a}$, $a_1 = (1-\phi)^2\left(\frac{N^c}{w_o}\right)^2 \frac{(\eta_1-\eta_{-1})^2}{3-2\phi}$, $a_2 = 0$, $a_4 = \frac{2(2-\phi)}{3-2\phi}\left[(1-\phi)N^c - \frac{\eta}{w_o}\right]$, $a_5 = 1$, and $a_3 = \frac{1}{3-2\phi}\left[\left[(1-\phi)N^c - \frac{\eta}{w_o}\right]^2 - 2(1-\phi)^2 N^c\left(\frac{\eta_{-1}+\eta_1}{w_o}\right)\right]$. For $\phi < 1$, Remark 2 does not hold in general. Indeed, it turns out that the extended model can admit up to three DFEs, so that, as in the SIR-Opinion model of Tyson et al. [22], the basic reproduction number depends on the initial distribution of the population along the attitude spectrum. Nevertheless, in the special case $\eta_{-1} = \eta_1$ (i.e. when the recruitment rates of individuals holding the two extreme opinions have the same shares in the total recruitment rate $\eta$) with opinion dynamics ($w_o > 0$), the extended SEIQR-Opinion model has a unique DFE where we have $S^c_{-1} = S^c_1 = \frac{1}{2}(N^c - S^c_0)$ and Equation (25b) is simplified to

$$S^c_0 = \frac{1}{3-2\phi}\left[(2-\phi)N^c + \frac{\eta}{w_o} - \sqrt{D_0}\right] \tag{25d}$$

with $D_0 = [(2-\phi)N^c + \eta/w_o]^2 - (3-2\phi)N^c(N^c + 2\eta_0/w_o)$. Here, the number $S^c_0$ of moderate opinion holders at the DFE increases not only with the baseline influence rate $w_o$ (as in Remark 2) but also with the influence rate reduction factor $\phi$. Hence the basic reproduction number $\mathcal{R}_0$ decreases with both $w_o$ and $\phi$. The study of the extended model can thus uncover interesting changes in opinion and disease dynamics.

**Funding:** This research received no external funding.

**Institutional Review Board Statement:** Not applicable.

**Data Availability Statement:** The authors confirm that the data supporting the findings of this work are available within the article.

**Conflicts of Interest:** The authors declare no conflict of interest.

## Appendix A. The Disease Dynamics Models

### *Appendix A.1. The Extended SEIQR Model*

The models considered for disease dynamics distinguish two different states during the pathogen incubation period when exposed individuals do not develop any COVID-19 symptoms: the simple Exposed ($E$) state for non-infectious individuals and the presymptomatic state ($I_p$) for infectious individuals. The simple exposition period lasts $1/\theta$ (up to 14 days [46], but generally short, i.e. about six days) and is followed by the presymptomatic period (which lasts $1/\sigma$) during which incubating individuals become infectious but remain

Preprints (www.preprints.org) | NOT PEER-REVIEWED | Posted: 5 December 2022 doi:10.20944/preprints202212.0067.v1



without symptom [45–50]. Contacts between susceptibles and presymptomatic infectious ($I_p$) can be sufficient for transmission (see e.g. [43] and [44]). When control measures such as contact tracing and systematic tests on target groups are implemented, some presymptomatic infectious are detected with probability $\pi$ and "quarantined" (i.e. isolated) at home, hospitals or dedicated places. The remaining (undetected) presymptomatic infectious individuals evolve into two groups based on the development or not of COVID-19 symptoms: $100\tau\%$ symptomatic infectious ($I_s$) and $100(1-\tau)\%$ asymptomatic infectious ($I_a$). Some symptomatic infectious individuals self-isolate or are detected and enter the class $Q$ of quarantined at the rate $\rho_s$. Again, contact tracing and systematic tests on target groups can lead to the detection and isolation of some asymptomatic infectious individuals at the rate $\rho_a$. Symptomatic infectious ($I_s$) and isolated individuals ($Q$) die of COVID-19 at the rates $\delta_s$ and $\delta_q$ respectively. The alive asymptomatic, symptomatic, and quarantined infectious individuals finally recover from COVID-19, at the rates $\gamma_a$, $\gamma_s$ and $\gamma_q$ respectively, and form the class of recovered individuals ($R$) who acquire a temporary immunity to SARS-CoV-2. Recovered individuals lose their immunity at the rate $\epsilon_o$ and become again susceptible to the pathogen. The flow diagram of the SEIQR model is depicted in Figure A1. The total population size $N(t)$ at time $t \geq 0$ is given by

$$N(t) = S(t) + E(t) + I_p(t) + I_a(t) + I_s(t) + Q(t) + R(t). \tag{A1}$$

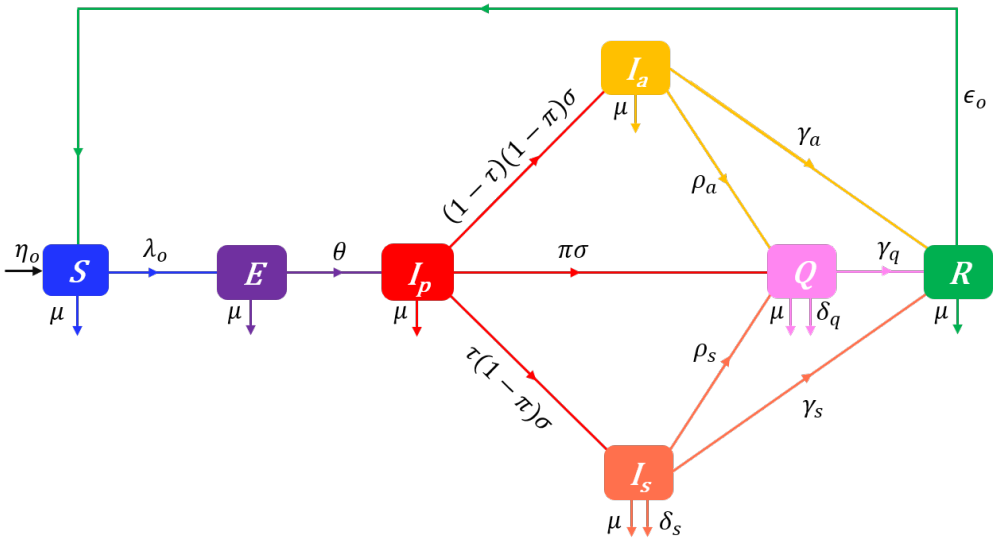


**Figure A1.** Flow-chart of a SEIQR model showing the flow of humans between different compartments. The susceptible population is denoted by $S$, and $E$, $I_p$, $I_a$, $I_s$, $Q$, and $R$ denote the exposed, the presymptomatic, the asymptomatic, the symptomatic, the quarantined infectious, and the recovered populations, respectively. The parameters of the model are described in Table 1.

The SEIQR model is described at time $t$ by the following system of differential equations:

$$\dot{S}(t) = \eta - \lambda_o(t)S(t) - \mu S(t) + \epsilon_o R(t), \tag{A2a}$$
$$\dot{E}(t) = \lambda_o(t)S(t) - (\theta + \mu)E(t), \tag{A2b}$$
$$\dot{I}_p(t) = \theta E(t) - (\sigma + \mu)I_p(t), \tag{A2c}$$
$$\dot{I}_a(t) = (1-\tau)(1-\pi)\sigma I_p(t) - (\rho_a + \gamma_a + \mu)I_a(t), \tag{A2d}$$
$$\dot{I}_s(t) = \tau(1-\pi)\sigma I_p(t) - (\rho_s + \gamma_s + \delta_s + \mu)I_s(t), \tag{A2e}$$
$$\dot{Q}(t) = \pi\sigma I_p(t) + \rho_a I_a(t) + \rho_s I_s(t) - (\gamma_q + \delta_q + \mu)Q(t), \tag{A2f}$$
$$\dot{R}(t) = \gamma_a I_a(t) + \gamma_s I_s(t) + \gamma_q Q(t) - (\epsilon_o + \mu)R(t), \tag{A2g}$$

Preprints (www.preprints.org) | NOT PEER-REVIEWED | Posted: 5 December 2022 doi:10.20944/preprints202212.0067.v1



with the nonnegative initial conditions $S(0) = S_0$, $E(0) = E_0$, $I_p(0) = I_{0p}$, $I_a(0) = I_{0a}$, $I_s(0) = I_{0s}$, $Q(0) = Q_0$, and $R(0) = R_0$ where $(S_0, E_0, I_{0p}, I_{0a}, I_{0s}, Q_0, R_0)^\top \in [0, \infty)^7$. In System (A2), $\lambda_o(t)$ is the force of infection, and the constant rate parameters of the model are described in Table 1.

*Appendix A.2. The UVEIQR Model*

Since many COVID-19 vaccines are currently distributed at various rates worldwide, we allow the disease dynamics model to account for vaccine-induced immunity. For simplicity, we do not distinguish age groups, although COVID-19 vaccination is widely implemented with different strategies and at different rates for children and adults [72–74]. Vaccines are primarily designed to prevent infectious diseases through the immunisation of vaccinated individuals [75,76], and thus increase the heterogeneity of the susceptible population $S$. Specifically, susceptible individuals are distinguished into an unvaccinated (and completely susceptible) population ($U$), which gets vaccinated at the rate $\upsilon$, and a vaccinated (with active vaccine-induced partial immunity) susceptible population ($V$), which loses vaccine-induced immunity at the rate $\alpha$ (the so-called re-susceptibility probability [77,78]). The timely number of net immigration (and new births) which enters the class of susceptibles is accordingly distinguished into unvaccinated ($\eta_u$) and vaccinated individuals ($\eta_v$) such that $\eta = \eta_u + \eta_v$. The flow diagram of the UVEIQR model is shown in Figure A2 and the disease dynamic is described by the following system of differential equations:

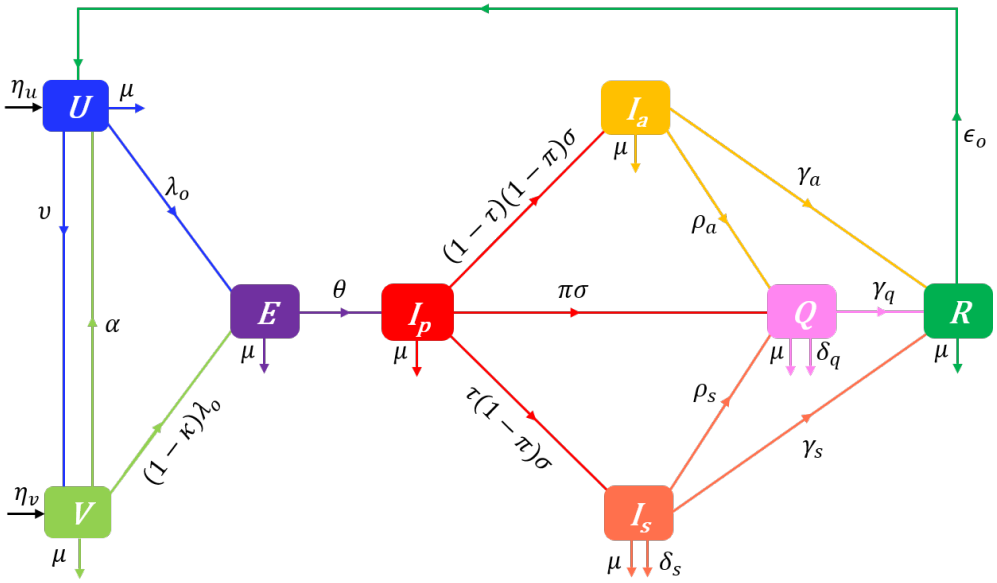


**Figure A2.** Flow-chart of a UVEIQR model showing the flow of humans between different compartments. $U$ is the unvaccinated (completely susceptible) population, $V$ is the healthy vaccinated but partially susceptible population, $E$, $I_p$, $I_a$, $I_s$, $Q$ and $R$ denote respectively the exposed, the presymptomatic infectious, the asymptomatic infectious, the symptomatic infectious, the quarantined, and the recovered populations. The parameters of the model are described in Table 1.

$$\dot{U}(t) = \eta_u - \upsilon U(t) + \alpha V(t) - \lambda_o(t)U(t) - \mu U(t) + \epsilon_o R(t), \tag{A3a}$$
$$\dot{V}(t) = \eta_v + \upsilon U(t) - \alpha V(t) - (1-\kappa)\lambda_o(t)V(t) - \mu V(t), \tag{A3b}$$
$$\dot{E}(t) = \lambda_o(t)U(t) + (1-\kappa)\lambda_o(t)V(t) - (\theta + \mu)E(t), \tag{A3c}$$
$$\dot{I}_p(t) = \theta E(t) - (\sigma + \mu)I_p(t), \tag{A3d}$$
$$\dot{I}_a(t) = (1-\tau)(1-\pi)\sigma I_p(t) - (\rho_a + \gamma_a + \mu)I_a(t), \tag{A3e}$$
$$\dot{I}_s(t) = \tau(1-\pi)\sigma I_p(t) - (\rho_s + \gamma_s + \delta_s + \mu)I_s(t), \tag{A3f}$$
$$\dot{Q}(t) = \pi\sigma I_p(t) + \rho_a I_a(t) + \rho_s I_s(t) - (\gamma_q + \delta_q + \mu)Q(t), \tag{A3g}$$
$$\dot{R}(t) = \gamma_a I_a(t) + \gamma_s I_s(t) + \gamma_q Q(t) - (\epsilon_o + \mu)R(t), \tag{A3h}$$

with the nonnegative initial conditions $U(0) = U_0$, $V(0) = V_0$, $E(0) = E_0$, $I_j(0) = I_{0j}$, $Q(0) = Q_0$, and $R(0) = R_0$ where $(U_0, V_0, E_0, Q_0, R_0)^\top \in [0, \infty)^5$ and $I_{0j} \geq 0$ for any $j \in \{p, a, s\}$. In System (A3), $\lambda_o(t)$ is the force of infection in the completely susceptible population as given by Equation (2), $\eta_u + \eta_v = \eta$, and the constant rate parameters are as described in Table 1. The total population size $N(t)$ is given at time $t$ by

$$N(t) = U(t) + V(t) + E(t) + I_p(t) + I_a(t) + I_s(t) + Q(t) + R(t).$$

Note that the UVEIQR model (A3) includes the SEIQR model (A2) as a special case when $V_0 = \upsilon = \eta_v = 0$ so that $V(t) = 0$ and $S(t) = U(t)$ for any $t \geq 0$. Also, note that for the general UVEIQR model, the force of infection is reduced by a factor $(1 - \kappa)$ in the vaccinated population.

*Appendix A.3. Mathematical Properties*

Since the SEIQR model (A2) is nested into the UVEIQR model (A3), we restrict attention to the latter, and then discuss the results in the special case $V_0 = \upsilon = \eta_v = 0$. The proofs of the results are given in Appendix C.1.

- *Non-negativity and Boundedness*

**Lemma A1** (Non-negativity and Boundedness)**.** *Under the nonnegative initial conditions $U(0) \geq 0$, $V(0) \geq 0$, $E(0) \geq 0$, $I_p(0) \geq 0$, $I_a(0) \geq 0$, $I_s(0) \geq 0$, $Q(0) \geq 0$ and $R(0) \geq 0$, all solutions of System (A3) remain nonnegative and are bounded for all $t > 0$.*

- *Disease-Free Equilibrium and Reproduction Number*

**Proposition A1** (Disease-Free Equilibrium & Reproduction Number)**.** *Set $p_v = \eta_v/\eta$. The UVEIQR model (A3) admits the unique disease-free equilibrium*

$$\boldsymbol{X}^c = (U^c, V^c, 0, 0, 0, 0, 0, 0)^\top \qquad \text{where} \tag{A4a}$$

$$U^c = \frac{\eta\alpha + \eta_u\mu}{\mu(\alpha + \upsilon + \mu)} \qquad \text{and} \qquad V^c = \frac{\eta\upsilon + \eta_v\mu}{\mu(\alpha + \upsilon + \mu)}, \tag{A4b}$$

*with the total population size at the carrying capacity $N^c = U^c + V^c = \eta/\mu$. Moreover, for a population described by System (A3), the basic reproduction number in a vaccination-free context (i.e. $V_0 = \eta_v = \upsilon = 0$) is given by*

$$\mathcal{R}_0 = \frac{\theta}{(\theta + \mu)(\sigma + \mu)}\left[\beta_p + \frac{(1-\tau)(1-\pi)\sigma}{\rho_a + \gamma_a + \mu}\beta_a + \frac{\tau(1-\pi)\sigma}{\rho_s + \gamma_s + \delta_s + \mu}\beta_s\right], \tag{A5a}$$

*and once vaccination is introduced, the control reproduction number is given by*

$$\mathcal{R}_c(\upsilon, \kappa, \alpha) = \mathcal{R}_0\left[1 - \frac{\kappa(\upsilon + p_v\mu)}{\alpha + \upsilon + \mu}\right] \tag{A5b}$$

*and satisfies*

$$(1 - \kappa)\mathcal{R}_0 \leq \mathcal{R}_c(\upsilon, \kappa, \alpha) \leq \mathcal{R}_0. \tag{A5c}$$

*The time-varying effective reproduction number is given by*

$$\mathcal{R}(t, \upsilon, \kappa, \alpha) = \mathcal{R}_0\left[\frac{U(t) + (1-\kappa)V(t)}{N(t) - Q(t)}\right]. \tag{A5d}$$

Note that the basic reproduction number $\mathcal{R}_0$ (A5) accounts for the implementation of a disease surveillance mechanism, if any (i.e. the detection rates $\pi$, $\rho_a$ and $\rho_s$ can be positive even in a disease-free context). In an emerging disease context (e.g. right before the report in late December 2020 of the first confirmed COVID-19 case), some symptoms

 doi:10.20944/preprints202212.0067.v1



might be unknown, and test kits might not be yet developed or available. In the special case where $\pi \approx \rho_a \approx \rho_s \approx 0$, the basic reproduction number is

$$\mathcal{R}_o = \frac{\theta}{(\theta+\mu)(\sigma+\mu)}\left[\beta_p + \frac{(1-\tau)\sigma}{\gamma_a+\mu}\beta_a + \frac{\tau\sigma}{\gamma_s+\delta_s+\mu}\beta_s\right] \tag{A6}$$

which satisfies $\mathcal{R}_0 \leq \mathcal{R}_o$ *ceteris paribus*. It appears from Equation (A5b) that, as expected, $\mathcal{R}_c$ decreases with both vaccination rate ($\upsilon$) and average vaccine efficacy ($\kappa$), but increases with the immunity lost rate ($\alpha$). The inequality (A5c) recognizes that vaccine efficacy is an important parameter in disease control: $\mathcal{R}_c$ cannot fall under $(1-\kappa)\mathcal{R}_0$ even for a large vaccination rate $\upsilon$. On setting

$$\kappa^* = \frac{\mathcal{R}_0 - 1}{\mathcal{R}_0} \tag{A7}$$

for $\mathcal{R}_0 > 1$, a necessary condition for disease eradication is that the average vaccine efficacy must satisfy $\kappa > \kappa^*$ (ensuring $(1-\kappa)\mathcal{R}_0 < 1$). The following corollary gives the critical vaccination rate to eradicate the disease for a fixed average vaccine efficacy $\kappa$.

**Corollary A1** (Critical Vaccination Rate)**.** *If $\mathcal{R}_0 > 1$ and $\kappa > \kappa^*$, then the critical (minimal) vaccination rate required to sufficiently lower $\mathcal{R}_c$ and ensure disease eradication in the long run is*

$$\upsilon^*(\kappa,\alpha) = \frac{(\alpha+\mu)(\mathcal{R}_0-1) - \kappa p_\upsilon \mu \mathcal{R}_0}{1-(1-\kappa)\mathcal{R}_0} \tag{A8a}$$

*which increases with the immunity lost rate $\alpha$, decreases with $\kappa$, and satisfies*

$$\upsilon^* > (\alpha+\mu)(\mathcal{R}_0-1) - p_\upsilon \mu \mathcal{R}_0. \tag{A8b}$$

Note that $\upsilon^*$ also decreases with $p_\upsilon$, so that a positive net immigration of vaccinated individuals lowers the minimal required vaccination rate. The following lemma establishes local asymptotic stability conditions for the disease-free equilibrium point and is further used to find global asymptotic stability conditions for the disease-free steady-state.

**Lemma A2** (Local Asymptotic Stability of the Disease-Free Equilibrium)**.** *The disease-free equilibrium $\boldsymbol{X}^c$ of the UVEIQR model (A3) is locally asymptotically stable if $\mathcal{R}_c \leq 1$, and unstable if $\mathcal{R}_c > 1$.*

**Proposition A2** (Global Asymptotic Stability of the Disease-Free Equilibrium)**.** *The disease-free equilibrium $\boldsymbol{X}^c$ of the UVEIQR model (A3) is globally asymptotically stable, i.e. $\lim_{t\to\infty} \boldsymbol{X}(t) = \boldsymbol{X}^c$ for any solution $\boldsymbol{X} = (U,V,E,I_p,I_a,I_s,Q,R)^\top$, provided that $\mathcal{R}_c \leq 1$.*

By Proposition A2, ensuring $\mathcal{R}_c < 1$ by for instance reducing contacts, susceptibility and transmissibility, or vaccinating a large part of the population, garrantees that the disease will die out shortly. If however $\mathcal{R}_c > 1$, then any introduction of infectious individuals has the potential to kick off and maintain an epidemic outbreak, as per the next lemma.

- *Persistence of the Disease and Endemic Equilibrium*

**Lemma A3** (Persistence of the Disease)**.** *Let us consider the UVEIQR model (A3) Let $\underline{U} = \eta_u/(\upsilon+\mu+\max\{\beta_p,\beta_a,\beta_s\})$. If $\mathcal{R}_c > 1$, then the disease persists uniformly, i.e. there exists a positive real constant $\varrho \in (0,\underline{U})$ independent of the initial data, such that any disease-dependent solution $\boldsymbol{X} = (U,V,E,I_p,I_a,I_s,Q,R)^\top$ satisfies:*

$$\lim_{t\to\infty} x(t) \geq \varrho \quad \text{for} \quad x \in \{U,E,I_p,I_a,I_s,Q,R\}, \tag{A9a}$$

$$\lim_{t\to\infty} V(t) \geq \varrho \quad \text{when} \quad \eta_\upsilon > 0 \quad \text{or} \quad \upsilon > 0, \quad \text{and} \tag{A9b}$$

$$\lim_{t\to\infty} V(t) = 0 \quad \text{when} \quad \eta_\upsilon = \upsilon = 0. \tag{A9c}$$

Preprints (www.preprints.org) | NOT PEER-REVIEWED | Posted: 5 December 2022 doi:10.20944/preprints202212.0067.v1



From Equation (A9a), it appears that in both vaccination-free (i.e. $\eta_v = \upsilon = 0$) and vaccination-dependent contexts, the susceptible population size $S(t) = U(t) + V(t)$ satisfies $\lim_{t\to\infty} S(t) \geq \varrho$ for any $\mathcal{R}_c > 0$ (since $\underline{U} < N^c$). This is ensured by the positive rates of net recruitment ($\eta_u > 0$), recovery ($\gamma_a, \gamma_s, \gamma_q > 0$), and immunity lost ($\alpha, \epsilon_o > 0$). The persistence of the disease when $\mathcal{R}_c > 1$ implies positive disease endemism whose equilibrium is next characterized.

**Proposition A3** (Endemic Equilibrium)**.** *If $\mathcal{R}_c \leq 1$, then the UVEIQR model (A3) has no endemic equilibrium. When $\mathcal{R}_c > 1$, the model admits the unique endemic equilibrium*

$$\boldsymbol{X}^\star = \left(U^\star, V^\star, E^\star, I_p^\star, I_a^\star, I_s^\star, Q^\star, R^\star\right)^\top \quad \text{with} \tag{A10a}$$

$$U^\star = \frac{[\alpha+\mu+(1-\kappa)\lambda_o^\star](\eta_u+\epsilon_o\theta d_p\sigma d_r E^\star)+\alpha\eta_v}{[\alpha+\mu+(1-\kappa)\lambda_o^\star](\upsilon+\mu+\lambda_o^\star)-\alpha\upsilon}, \tag{A10b}$$

$$V^\star = \frac{\eta_v+\upsilon U^\star}{\alpha+\mu+(1-\kappa)\lambda_o^\star}, \tag{A10c}$$

$$E^\star = \frac{\bar{S}^c N^c}{\mathcal{R}_c(\theta+\mu)+\bar{S}^c\theta d_m\lambda_o^\star}\lambda_o^\star, \tag{A10d}$$

$$I_p^\star = \theta d_p E^\star, \tag{A10e}$$

$$I_a^\star = \theta d_p\sigma d_a E^\star, \tag{A10f}$$

$$I_s^\star = \theta d_p\sigma d_s E^\star, \tag{A10g}$$

$$Q^\star = \theta d_p\sigma d_q E^\star, \tag{A10h}$$

$$R^\star = \theta d_p\sigma d_r E^\star, \tag{A10i}$$

*where we have set $d_p = \frac{1}{\sigma+\mu}$, $d_a = \frac{(1-\tau)(1-\pi)}{\rho_a+\gamma_a+\mu}$, $d_s = \frac{\tau(1-\pi)}{\rho_s+\gamma_s+\delta_s+\mu}$, $d_q = \frac{\pi+d_a\rho_a+d_s\rho_s}{\gamma_q+\delta_q+\mu}$, $d_r = \frac{d_a\gamma_a+d_s\gamma_s+d_q\gamma_q}{\epsilon_o+\mu}$, $d_m = d_n + d_p\sigma d_q$, $d_n = \frac{d_p\sigma}{\mu}(d_s\delta_s + d_q\delta_q)$, and $\bar{S}^c = 1 - \frac{\kappa(\upsilon+p_v\mu)}{\alpha+\upsilon+\mu}$; the endemic force of infection $\lambda_o^\star$ is given by*

$$\lambda_o^\star = \frac{1}{2}\left(\sqrt{K_1^2+4K_0}-K_1\right) \quad \text{where} \tag{A10j}$$

$$K_0 = \frac{\mu(\alpha+\upsilon+\mu)(\theta+\mu)(\mathcal{R}_c-1)}{(1-\kappa)[(\theta+\mu)-\theta(d_m\mu+d_p\sigma d_r\epsilon_o)]}, \quad \text{and}$$

$$K_1 = \frac{(\theta+\mu)[g_{uv}+(1-\kappa)\mu]-\theta(d_m\mu+d_p\sigma d_r\epsilon_o)g_{uv}-(1-\kappa)\theta d_p\mu\beta_\sigma+\kappa p_v\theta d_m\mu^2}{(1-\kappa)[(\theta+\mu)-\theta(d_m\mu+d_p\sigma d_r\epsilon_o)]}$$

*with $g_{uv} = \alpha+(1-\kappa)\upsilon+\mu$, and $\beta_\sigma = \beta_p+\sigma d_a\beta_a+\sigma d_s\beta_s$; and the total population size is*

$$N^\star = N^c - \theta d_n E^\star. \tag{A10k}$$

The following results establish stability for the endemic equilibrium $\boldsymbol{X}^\star$.

**Lemma A4** (Local Asymptotic Stability of the Endemic Equilibrium)**.** *When it exists ($\mathcal{R}_c > 1$), the endemic equilibrium $\boldsymbol{X}^\star$ of the UVEIQR model (A3) is locally asymptotically stable.*

**Proposition A4** (Global Asymptotic Stability of the Endemic Equilibrium)**.** *When it exists, the endemic equilibrium $\boldsymbol{X}^\star$ of the UVEIQR model (A3) is globally asymptotically stable, i.e. $\lim_{t\to\infty}\boldsymbol{X}(t) = \boldsymbol{X}^\star$ for any disease-dependent solution $\boldsymbol{X} = (U, V, E, I_p, I_a, I_s, Q, R)^\top$.*

Note from Proposition A4 and Equation (A10k) that the persistence of disease ($\mathcal{R}_c > 1$) and the positif disease related death rates ($\delta_s, \delta_q > 0$) reduce the long run population size below the carrying capacity $N^c$.

Preprints (www.preprints.org) | NOT PEER-REVIEWED | Posted: 5 December 2022 doi:10.20944/preprints202212.0067.v1



## Appendix B. Overview of Fixed-order Saturating Influence Functions

### *Appendix B.1. Vaccination–free Influence Functions*

Plot the 3 influences for $w_\infty = 1, 2, 3$.

### *Appendix B.2. Influence functions accounting for vaccination*

Build 3D plots of influences in terms of $\widetilde{P}$ and $V$ to support the claims.

Compare the concavity or convexity of different types of influence functions.

## Appendix C. Proofs of Lemmas and Propositions

### *Appendix C.1. Proofs of Lemmas and Propositions Related to Disease Dynamics Only*

**Proof of Lemma A1.** From Equation (A3a), we have $\dot{U}(t) \geq -(\upsilon + \tilde{\beta} + \mu)U(t)$ where $\tilde{\beta} = \max\{\beta_p, \beta_a, \beta_s\}$ (note from Equation (2) that $\tilde{\beta}$ is a majorant of $\lambda_o(t)$). This leads to:

$$U(t) \geq U_0 e^{-(\upsilon+\tilde{\beta}+\mu)t} \geq 0.$$

The same argument gives $V(t) \geq 0$, $E(t) \geq 0$, $I_p(t) \geq 0$, $I_a(t) \geq 0$, $I_s(t) \geq 0$, $Q(t) \geq 0$ and $R(t) \geq 0$ and proves nonnegativity. Next, let $N_0 = N(0)$. Then, by the nonnegative initial conditions and $N_0 = U_0 + V_0 + E_0 + I_{0p} + I_{0a} + I_{0s} + Q_0 + R_0$, we have $N_0 \geq 0$. From Equation (1) and the System (A3), we have

$$\dot{N}(t) = \eta - \mu N(t) - \delta_s I_s(t) - \delta_q Q(t).$$

The last equation implies that $\dot{N}(t) \leq \eta - \mu N(t)$. Integrating the later yields

$$N(t) \leq N^c + (N_0 - N^c)e^{-\mu t}$$

with $N^c = \eta/\mu$. It appears that as $t$ increases, the upper bound of $N(t)$ increases (when $N_0 \leq N^c$) or decreases (when $N_0 > N^c$) to eventually approach the carrying capacity $N^c$ as $t \to \infty$. Thus $N(t) \leq \max\{N_0, N^c\}$. Hence we overall have

$$0 \leq N(t) \leq \max\{N_0, N^c\}.$$

The nonnegativity of $U(t)$, $V(t)$, $E(t)$, $I_p(t)$, $I_a(t)$, $I_s(t)$, $Q(t)$ and $R(t)$ then implies that these quantities are all bounded, since their sum $N(t)$ is bounded. □

**Proof of Proposition A1.** Adding the disease-free restriction $E = I_p = I_a = I_s = Q = 0$ to System (A3) implies that $\lambda_o(t) = 0$. Setting all the derivatives to zero then gives $E^c = I_p^c = I_a^c = I_s^c = Q^c = R^c = 0$ and we are left with the system

$$\begin{cases} \eta_u & - & (\upsilon+\mu)U^c & + & \alpha V^c & = 0 \\ \eta_v & + & \upsilon U^c & - & (\alpha+\mu)V^c & = 0 \end{cases}$$

which is solved for $U^c$ and $V^c$ through substitution, and the disease-free equilibrium (d.f.e.) in Equation (A4a) is obtained using $\eta = \eta_u + \eta_v$. Next, let $\boldsymbol{I}$ the vector of the compartments involved in the production of new infections or receiving new infections: $\boldsymbol{I} = (E, I_p, I_a, I_s)$. The corresponding subset of System (A3) has the form $\dot{\boldsymbol{I}} = \mathbb{F}(\boldsymbol{I}) - \mathbb{W}(\boldsymbol{I})$ where

$$\mathbb{F}(\boldsymbol{I}) = \bar{S}\begin{pmatrix} \beta_p I_p + \beta_a I_a + \beta_s I_s \\ 0 \\ 0 \\ 0 \end{pmatrix} \quad \text{and} \quad \mathbb{W}(\boldsymbol{I}) = \begin{pmatrix} (\theta+\mu)E \\ -\theta E + (\sigma+\mu)I_p \\ -(1-\tau)(1-\pi)\sigma I_p + (\rho_a+\gamma_a+\mu)I_a \\ -\tau(1-\pi)\sigma I_p + (\rho_s+\gamma_s+\delta_s+\mu)I_s \end{pmatrix}$$

Preprints (www.preprints.org) | NOT PEER-REVIEWED | Posted: 5 December 2022 doi:10.20944/preprints202212.0067.v1



on setting $\bar{S} = \frac{U+(1-\kappa)V}{N-Q}$. Then, letting $g_e = \theta + \mu$, $g_p = \sigma + \mu$, $g_a = \rho_a + \gamma_a + \mu$, $g_s = \rho_s + \gamma_s + \delta_s + \mu$, $f_a = (1-\tau)(1-\pi)\sigma$, and $f_s = \tau(1-\pi)\sigma$, the Jacobian matrices of $\mathbb{F}$ and $\mathbb{W}$ evaluated at the d.f.e. are respectively given by

$$\boldsymbol{F}^c = \bar{S}^c \begin{pmatrix} 0 & \beta_p & \beta_a & \beta_s \\ 0 & 0 & 0 & 0 \\ 0 & 0 & 0 & 0 \\ 0 & 0 & 0 & 0 \end{pmatrix} \text{ and } \boldsymbol{W} = \begin{pmatrix} g_e & 0 & 0 & 0 \\ -\theta & g_p & 0 & 0 \\ 0 & -f_a & g_a & 0 \\ 0 & -f_s & 0 & g_s \end{pmatrix} \text{ with } \bar{S}^c = \frac{U^c + (1-\kappa)V^c}{N^c - Q^c}.$$

Following [63], the basic reproduction number is the spectral radius (largest eigenvalue) of the next-generation matrix $\boldsymbol{F}^c\boldsymbol{W}^{-1}$:

$$\boldsymbol{s}_\rho\left(\boldsymbol{F}^c\boldsymbol{W}^{-1}\right) = \frac{\theta}{g_e g_p}\left[\beta_p + \frac{f_a}{g_a}\beta_a + \frac{f_s}{g_s}\beta_s\right]\bar{S}^c.$$

Under the restriction $V_0 = \eta_v = \upsilon = 0$, we have $V^c = 0$ and $U^c = N^c$. We thus have in this case $\bar{S}^c = 1$ (since $Q^c = 0$), and Equation (A5a) follows. Using the Equations in (A4b) gives $\bar{S}^c = \frac{\eta\alpha + \eta_u\mu + (1-\kappa)(\eta\upsilon + \eta_v\mu)}{\eta(\alpha+\upsilon+\mu)}$ and Equation (A5b) follows. The expression (A5c) results from noting that $\mathcal{R}_c(\upsilon, \kappa, \alpha)$ decreases with $\kappa$ and evaluating the limit $\mathcal{R}_c(\upsilon, 0, \alpha)$ to get an upper bound, and noting that $\mathcal{R}_c$ also decreases with $\upsilon$ since $\frac{\partial \mathcal{R}_c(\upsilon,\kappa,\alpha)}{\partial \upsilon} = -\mathcal{R}_0 \frac{\kappa(\alpha+\mu(1-p_v))}{\alpha+\upsilon+\mu} < 0$, and evaluating the limit $\mathcal{R}_c(\infty, \kappa, \alpha)$ to obtain a lower bound. Finally, evaluating the Jacobian matrices of $\mathbb{F}$ and $\mathbb{W}$ at general values of $U$, $V$, $Q$, and $N$ instead of the d.f.e. (i.e. replacing $\bar{S}^c$ by $\bar{S}$), results in Equation (A5d). □

**Proof of Corollary A1.** We obtain $\upsilon^*(\kappa, \alpha)$ by setting the expression (A5b) of $\mathcal{R}_c$ to one, and solving for $\upsilon$. It is obvious that $\upsilon^*$ increases with $\alpha$. From Equation (A8a), we get

$$\frac{\partial \upsilon^*(\kappa, \alpha)}{\partial \kappa} = -\frac{[\alpha + \mu(1-p_v)](\mathcal{R}_0 - 1)\mathcal{R}_0}{[1-(1-\kappa)\mathcal{R}_0]^2} < 0,$$

hence $\upsilon^*(\kappa, \alpha)$ decreases with $\kappa \in (0, 1)$, and is lower bounded by $\upsilon^*(1, \alpha)$. □

**Proof of Lemma A2.** A necessary and sufficient condition for an equilibrium to have local asymptotic stability (l.a.s.) is that all eigenvalues of the Jacobian matrix have negative real parts [79]. The Jacobian matrix of the model (A3) at the d.f.e. has the block structure

$$\boldsymbol{J}^c = \begin{pmatrix} \boldsymbol{J}_S & \boldsymbol{J}^c_{SI} & \boldsymbol{J}_{SQ} \\ \boldsymbol{0} & \boldsymbol{J}^c_I & \boldsymbol{0} \\ \boldsymbol{0} & \boldsymbol{J}_{QI} & \boldsymbol{J}_Q \end{pmatrix} \quad \text{where} \quad \boldsymbol{J}_S = \begin{pmatrix} -(\upsilon+\mu) & \alpha \\ \upsilon & -(\alpha+\mu) \end{pmatrix},$$

$\boldsymbol{J}^c_{SI} = \frac{-1}{N^c}\begin{pmatrix} 0 & \beta_p U^c & \beta_a U^c & \beta_s U^c \\ 0 & (1-\kappa)\beta_p V^c & (1-\kappa)\beta_a V^c & (1-\kappa)\beta_s V^c \end{pmatrix}$, $\boldsymbol{J}_{SQ} = \begin{pmatrix} 0 & \epsilon_o \\ 0 & 0 \end{pmatrix}$, $\boldsymbol{J}^c_I = \boldsymbol{F}^c - \boldsymbol{W}$, $\boldsymbol{J}^c_{QI} = \begin{pmatrix} 0 & \pi\sigma & \rho_a & \rho_s \\ 0 & 0 & \gamma_a & \gamma_s \end{pmatrix}$, and $\boldsymbol{J}_Q = \begin{pmatrix} -(\gamma_q + \delta_q + \mu) & 0 \\ \gamma_q & -(\epsilon_o + \mu) \end{pmatrix}$. From this structure, the eigenvalues of $\boldsymbol{J}^c$ are those of $\boldsymbol{J}_S$, $\boldsymbol{J}^c_I$ and $\boldsymbol{J}_Q$ (using Schur complements). We get the eigenvalues $d_1 = -\mu$ and $d_2 = -(\upsilon + \alpha + \mu)$ from $\boldsymbol{J}_S$, and $d_3 = -(\gamma_q + \delta_q + \mu)$ and $d_4 = -(\epsilon_o + \mu)$ from $\boldsymbol{J}_Q$. Since $d_k < 0$ for $k = 1, 2, 3, 4$, we can next restrict attention to $\boldsymbol{J}^c_I$ whose four eigenvalues must have negative real parts to ensure l.a.s.:

$$\boldsymbol{J}^c_I = \begin{pmatrix} -g_e & \bar{S}^c\beta_p & \bar{S}^c\beta_a & \bar{S}^c\beta_s \\ \theta & -g_p & 0 & 0 \\ 0 & f_a & -g_a & 0 \\ 0 & f_s & 0 & -g_s \end{pmatrix}.$$

The characteristic polynomial $P_c$ of $\boldsymbol{J}^c_I$ is

$$P_c(d) = d^4 + K_3 d^3 + K_2 d^2 + K_1 d + g_e g_p g_a g_s (1 - \mathcal{R}_c),$$

Preprints (www.preprints.org) | NOT PEER-REVIEWED | Posted: 5 December 2022 doi:10.20944/preprints202212.0067.v1



where $K_3 = g_e + g_p + g_a + g_s$, $K_2 = g_e(g_p + g_a + g_s) + g_p(g_a + g_s) + g_a g_s - \theta \bar{S}^c \beta_p$, and $K_1 = g_e g_p(g_a + g_s) + g_a g_s(g_e + g_p) - \theta \bar{S}^c[(g_a + g_s)\beta_p + f_a\beta_a + f_s\beta_s]$. The Routh-Hurwitz stability conditions (see Equation (A.22) in May [80, page 196]) corresponding to this polynomial are:

$$K_3 > 0, \quad K_1 > 0, \quad \text{and} \quad K_c \geq 0,$$

where $K_c = g_e g_p g_a g_s(1 - \mathcal{R}_c)$. Since $g_j > 0$ for any $j \in \{e, p, a, s\}$, we have (i): $K_3 > 0$ by definition (for any value of $\mathcal{R}_c$). If $\mathcal{R}_c > 1$, then $K_c < 0$. It follows that at least one eigenvalue of $\boldsymbol{J}_I^c$ has a positive real part when $\mathcal{R}_c > 1$, and instability is established. When $\mathcal{R}_c \leq 1$ on the contrary, we have (ii): $K_c \geq 0$. Next, notice that $\mathcal{R}_c \leq 1$ is equivalent to $1 \geq \frac{\theta \bar{S}^c}{g_e g_p}\left(\beta_p + \frac{f_a}{g_a}\beta_a + \frac{f_s}{g_s}\beta_s\right)$. This implies that $1 > \frac{\theta \bar{S}^c}{g_e g_p}\left(\beta_p + \frac{f_a}{g_a+g_s}\beta_a + \frac{f_s}{g_a+g_s}\beta_s\right)$ since $g_a > 0$ and $g_s > 0$. Writing $K_1$ as

$$K_1 = g_e g_p(g_a + g_s)\left[1 - \frac{\theta \bar{S}^c}{g_e g_p}\left(\beta_p + \frac{f_a}{g_a + g_s}\beta_a + \frac{f_s}{g_a + g_s}\beta_s\right)\right] + g_a g_s(g_e + g_p),$$

then shows that (iii): $K_1 > 0$ if $\mathcal{R}_c \leq 1$. The statements (i), (ii) and (iii) ensure that all the four eigenvalues of $\boldsymbol{J}_I^c$ have negative real parts when $\mathcal{R}_c \leq 1$ and l.a.s. is established. □

**Proof of Proposition A2.** The proof uses a global stability result from Castillo-Chavez et al. [81]. Let $\boldsymbol{Y} = (U, V, R)^\top$ and $\boldsymbol{I} = (E, I_p, I_a, I_s, Q)^\top$ be the vectors of uninfected and infected classes, respectively, and set $\boldsymbol{G}(\boldsymbol{Y}, \boldsymbol{I}) = \frac{\partial \boldsymbol{I}(t)}{\partial t}$ and $\boldsymbol{Y}^c = (U^c, V^c, 0)^\top$. To establish global asymptotic stability (g.a.s.), we first show that the following conditions hold for the UVEIQR model (A3):

$$(H_1): \quad \lim_{t\to\infty} \boldsymbol{Y}(t) = \boldsymbol{Y}^c \quad \text{(i.e. } \boldsymbol{Y}^c \text{ is globally asymptotically stable) when } \boldsymbol{I} = \boldsymbol{0},$$
$$(H_2): \quad \boldsymbol{G}(\boldsymbol{Y}, \boldsymbol{I}) = \boldsymbol{A}^c \boldsymbol{I} - \widehat{\boldsymbol{G}}(\boldsymbol{Y}, \boldsymbol{I}), \quad \widehat{\boldsymbol{G}}(\boldsymbol{Y}, \boldsymbol{I}) \geq \boldsymbol{0} \quad \text{(i.e. all entries of } \widehat{\boldsymbol{G}} \text{ are nonnegative)},$$

where $\boldsymbol{A}^c = \partial \boldsymbol{G}(\boldsymbol{Y}^c, \boldsymbol{0})/\partial \boldsymbol{I}^\top$ is a Metzeler matrix (all off-diagonal elements are nonnegative). To check $(H_1)$, we set $\boldsymbol{I} = \boldsymbol{0}$ in System (A3) and get the reduced system

$$\begin{aligned}
\dot{U} &= \eta_u - (\upsilon + \mu)U + \alpha V + \epsilon_o R,\\
\dot{V} &= \eta_v + \upsilon U - (\alpha + \mu)V,\\
\dot{R} &= -(\epsilon_o + \mu)R.
\end{aligned}$$

It comes that $R(t) = R_0 \mathrm{e}^{-(\epsilon_o+\mu)t}$, and $N(t) = N^c + (N_0 - N^c)\mathrm{e}^{-\mu t}$. Replacing the expression $U(t) = N(t) - R(t) - V(t)$ in $\dot{V}(t)$ and integrating the result leads to

$$\begin{aligned}
V(t) = V_0 \mathrm{e}^{-(\alpha+\upsilon+\mu)t} &+ \frac{\eta_v + \upsilon N^c}{\alpha + \upsilon + \mu}\left[1 - \mathrm{e}^{-(\alpha+\upsilon+\mu)t}\right] + \frac{\upsilon(N_0 - N^c)}{\alpha + \upsilon}\left[1 - \mathrm{e}^{-(\alpha+\upsilon)t}\right]\mathrm{e}^{-\mu t}\\
&- \upsilon R_0 \cdot t \cdot \mathrm{e}^{-(\alpha+\upsilon+\mu)t} \qquad \text{if } \alpha + \upsilon = \epsilon_o \quad \text{and}\\
V(t) = V_0 \mathrm{e}^{-(\alpha+\upsilon+\mu)t} &+ \frac{\eta_v + \upsilon N^c}{\alpha + \upsilon + \mu}\left[1 - \mathrm{e}^{-(\alpha+\upsilon+\mu)t}\right] + \frac{\upsilon(N_0 - N^c)}{\alpha + \upsilon}\left[1 - \mathrm{e}^{-(\alpha+\upsilon)t}\right]\mathrm{e}^{-\mu t}\\
&- \frac{\upsilon R_0}{\alpha + \upsilon - \epsilon_o}\left[\mathrm{e}^{-\epsilon_o t} - \mathrm{e}^{-(\alpha+\upsilon)t}\right]\mathrm{e}^{-\mu t} \qquad \text{if } \alpha + \upsilon \neq \epsilon_o.
\end{aligned}$$

It appears that $\lim_{t\to\infty} R(t) = 0 = R^c$ and $\lim_{t\to\infty} V(t) = \frac{\eta_v + \upsilon N^c}{\alpha+\upsilon+\mu} = V^c$, both when $\alpha + \upsilon = \epsilon_o$ (since $\alpha + \upsilon + \mu > 0$) and when $\alpha + \upsilon \neq \epsilon_o$. Then, $U(t) = N(t) - R(t) - V(t)$

Preprints (www.preprints.org) | NOT PEER-REVIEWED | Posted: 5 December 2022 doi:10.20944/preprints202212.0067.v1



leads to $\lim_{t\to\infty} U(t) = N^c - V^c - R^c = U^c$, hence $(H_1)$ holds. Next, using System (A3) and $\widehat{\boldsymbol{G}}(\boldsymbol{Y},\boldsymbol{I}) = \boldsymbol{A}^c\boldsymbol{I} - \boldsymbol{G}(\boldsymbol{Y},\boldsymbol{I})$, and setting $g_q = \gamma_q + \delta_q + \mu$, we get

$$\boldsymbol{A}^c = \begin{pmatrix} -g_e & \bar{S}^c\beta_p & \bar{S}^c\beta_a & \bar{S}^c\beta_s & 0 \\ \theta & -g_p & 0 & 0 & 0 \\ 0 & f_a & -g_a & 0 & 0 \\ 0 & f_s & 0 & -g_s & 0 \\ 0 & \pi\sigma & \rho_a & \rho_s & -g_q \end{pmatrix} \text{ and } \widehat{\boldsymbol{G}}(\boldsymbol{Y},\boldsymbol{I}) = (\bar{S}^c - \bar{S}) \begin{pmatrix} \beta_p I_p + \beta_a I_a + \beta_s I_s \\ 0 \\ 0 \\ 0 \\ 0 \end{pmatrix}.$$

The matrix $\boldsymbol{A}^c$ is obviously Metzeler. Moreover, the whole population is in the susceptible class $S$ at the d.f.e., hence the maximal value of the average effective susceptibility in the mixing population $\bar{S} = \frac{U+(1-\kappa)V}{N-Q}$, is $\bar{S}^c = \frac{U^c+(1-\kappa)V^c}{N^c}$. We thus have $\bar{S}^c \geq \bar{S}$ and $\widehat{\boldsymbol{G}}(\boldsymbol{Y},\boldsymbol{I}) \geq 0$ so that $(H_2)$ holds. Then, by the Theorem in [81], the validity of the two conditions ($(H_1)$ and $(H_2)$) ensures that the d.f.e. $\boldsymbol{X}^c$ is g.a.s. provided that $\boldsymbol{X}^c$ is l.a.s., i.e. $\mathcal{R}_c \leq 1$ (by Lemma A2). □

**Proof of Lemma A3.** The proof is an adaptation of the proof of Theorem 3.3 in [82], initially built for dissipative dynamical systems. The primary aim is to find a positive sub-solution of the UVEIQR model (A3). Let $\boldsymbol{I} = (E, I_p, I_a, I_s)^\top$ and set $\boldsymbol{G}(t,\boldsymbol{I}) = \frac{\partial \boldsymbol{I}(t)}{\partial t}$. Note that the subset of System (A3) corresponding to $\boldsymbol{I}$ (i.e. Equations (A3c)–(A3f)) can be compactly expressed as $\dot{\boldsymbol{I}} = \boldsymbol{G}(t,\boldsymbol{I})$. We first show the existence of a pair of positive principal eigenvalue and eigenvector of this subset when $\mathcal{R}_c > 1$. Linearizing the target subset of the system around the d.f.e. $\boldsymbol{X}^c$ gives $\dot{\boldsymbol{I}} = \boldsymbol{A}^c\boldsymbol{I}$, where $\boldsymbol{A}^c = \partial\boldsymbol{G}(t,\boldsymbol{0})/\partial\boldsymbol{I}^\top$, i.e.

$$\boldsymbol{A}^c = \begin{pmatrix} -g_e & \bar{S}^c\beta_p & \bar{S}^c\beta_a & \bar{S}^c\beta_s \\ \theta & -g_p & 0 & 0 \\ 0 & f_a & -g_a & 0 \\ 0 & f_s & 0 & -g_s \end{pmatrix}.$$

Substituting a solution of the form $\boldsymbol{I}(t) = \boldsymbol{\Phi}\mathrm{e}^{d\times t}$ with $d \in \mathbb{R}$, we get $d\boldsymbol{\Phi} = \boldsymbol{A}^c\boldsymbol{\Phi}$. Note that $\boldsymbol{A}^c$ is a Metzeler matrix (i.e. $(\boldsymbol{A}^c)_{ij} \geq 0$ for $i \neq j$). Therefore, $\boldsymbol{A}^c$ is irreducible if and only if the matrix $\boldsymbol{A}_+ = \boldsymbol{A}^c + c\boldsymbol{I}_6$ (with $c$ any large real such that $(\boldsymbol{A}_+)_{ij} \geq 0$ for $1 \leq i,j, \leq 4$) is irreducible [83]. We pick $c = \nu + \max\{g_e, g_p, g_a, g_s, g_q, g_r\}$ with $\nu$ a positive real, and let $\bar{g}_j = c + g_j \geq \nu > 0$ for $j \in \{e,p,a,s,q,r\}$. Then,

$$\boldsymbol{A}_+ = \begin{pmatrix} \bar{g}_e & \bar{S}^c\beta_p & \bar{S}^c\beta_a & \bar{S}^c\beta_s \\ \theta & \bar{g}_p & 0 & 0 \\ 0 & f_a & \bar{g}_a & 0 \\ 0 & f_s & 0 & \bar{g}_s \end{pmatrix}, \text{ and}$$

$$\boldsymbol{A}_+^2 = \begin{pmatrix} \bar{g}_e^2 + \theta\bar{S}^c\beta_p & \bar{S}^c\bar{g}_e\beta_p + \bar{g}_p\beta_p + f_a\beta_a + f_s\beta_s & \bar{S}^c\beta_a(\bar{g}_e + \bar{g}_a) & \bar{S}^c\beta_s(\bar{g}_e + \bar{g}_s) \\ \theta(\bar{g}_e + \bar{g}_p) & \bar{g}_p^2 + \theta\bar{S}^c\beta_p & \theta\bar{S}^c\beta_a & \theta\bar{S}^c\beta_s \\ \theta f_a & f_a(\bar{g}_p + \bar{g}_a) & \bar{g}_a^2 & 0 \\ \theta f_s & f_s(\bar{g}_p + \bar{g}_s) & 0 & \bar{g}_s^2 \end{pmatrix}.$$

We observe that $(\boldsymbol{A}_+^2)_{34} = (\boldsymbol{A}_+^2)_{43} = 0$. However, it appears that the corresponding elements in $\boldsymbol{A}_+^3$ are positive, and therefore $\boldsymbol{A}_+^3 \gg 0$ (all elements are positive), so that $\boldsymbol{A}_+$ is irreducible. It follows that $\boldsymbol{A}^c$ is irreducible, and by Corollary 4.3.2 in [83], there exists a real eigenvalue $\tilde{d}$ of $\boldsymbol{A}^c$ and a corresponding eigenvector $\tilde{\boldsymbol{\Phi}} = \left(\tilde{E}, \tilde{I}_p, \tilde{I}_a, \tilde{I}_s\right)^\top$ satisfying $\tilde{\boldsymbol{\Phi}} \gg 0$. Since $\mathcal{R}_c > 1$, the principal eigenvalue $\tilde{d}$ of $\boldsymbol{A}^c$ is positive (by Lemma A2).

To find a sub-solution of System (A3), notice that by Lemma A2, any solution of the system satisfies $\lim_{t\to\infty} \boldsymbol{X} \neq \boldsymbol{X}^c$ (since $\mathcal{R}_c > 1$). Along with the irreducibility of $\boldsymbol{A}^c$, this implies that, in the presence of the disease, for a small constant $\nu > 0$, there

Preprints (www.preprints.org) | NOT PEER-REVIEWED | Posted: 5 December 2022 doi:10.20944/preprints202212.0067.v1



exists a large time $T$ such that $0 < E(t), I_p(t), I_a(t), I_s(t) \leq \nu$ for $t \geq T$. On setting $\tilde{\mu} = \mu + \max\{\beta_p, \beta_a, \beta_s\}$ and $\tilde{g}_u = \upsilon + \tilde{\mu}$, the solution to the Cauchy problem

$$\begin{cases} \frac{\partial U_b(t)}{\partial t} = & \eta_u & - & \tilde{g}_u U_b(t), & t \geq T, \\ U_b(T) = & U(T), & & & \end{cases}$$

is a sub-solution of Equation (A3a). We find $U_b(t) = \underline{U} + [U(T) - \underline{U}]\mathrm{e}^{-\tilde{g}_u(t-T)}$ with $\underline{U} = \eta_u/\tilde{g}_u > 0$, hence $\lim_{t\to\infty} U_b(t) = \underline{U}$. Similarly, on setting $\tilde{\eta}_v = \eta_v + \upsilon\tilde{\underline{U}}$ with $\tilde{\underline{U}} = \min\{\underline{U}, U(T)\}$, and $\tilde{g}_v = \alpha + \tilde{\mu}$, a sub-solution of Equation (A3b) is given by the solution of the Cauchy problem,

$$\begin{cases} \frac{\partial V_b(t)}{\partial t} & = & \tilde{\eta}_v & - & \tilde{g}_v V_b(t), & t \geq T, \\ V_b(T) & = & V(T). & & & \end{cases}$$

We find $\lim_{t\to\infty} V_b(t) = \underline{V}$ with $\underline{V} = \tilde{\eta}_v/\tilde{g}_v \geq 0$. Next, let $\tilde{\boldsymbol{I}}(t) = \tilde{\nu}\tilde{\boldsymbol{\Phi}}$ for $t \geq T$ and $\tilde{\nu} > 0$ a small constant. Substituting $\tilde{\boldsymbol{I}}(t)$ into Equations (A3c)–(A3f), exploiting the positivity of $\tilde{d}$ and $\tilde{\boldsymbol{\Phi}} = \big(\tilde{E}, \tilde{I}_p, \tilde{I}_a, \tilde{I}_s\big)^\top$, and setting $\tilde{a} = \tilde{E} + \tilde{I}_p + \tilde{I}_a + \tilde{I}_s + R$ result in:

$$\begin{aligned}
\dot{E}(t) - \frac{\partial(\tilde{\nu}\tilde{E})}{\partial t} &= \tilde{\nu}(\beta_p\tilde{I}_p + \beta_a\tilde{I}_a + \beta_s\tilde{I}_s)\frac{U + (1-\kappa)V}{U + V + \tilde{\nu}(\tilde{E} + \tilde{I}_p + \tilde{I}_a + \tilde{I}_s + R)} - \tilde{\nu}g_e\tilde{E}, \\
&= \tilde{\nu}(\beta_p\tilde{I}_p + \beta_a\tilde{I}_a + \beta_s\tilde{I}_s)\frac{U + (1-\kappa)V}{U + V + \tilde{\nu}\tilde{a}} - \tilde{\nu}g_e\tilde{E} \\
&\quad + \tilde{\nu}\big(\beta_p\tilde{I}_p - \beta_p\tilde{I}_p + \beta_a\tilde{I}_a - \beta_a\tilde{I}_a + \beta_s\tilde{I}_s - \beta_s\tilde{I}_s\big)\bar{S}^c, \\
&= \tilde{\nu}\big[(\beta_p\tilde{I}_p + \beta_a\tilde{I}_a + \beta_s\tilde{I}_s)\bar{S}^c - g_e\tilde{E}\big] \\
&\quad + \tilde{\nu}(\beta_p\tilde{I}_p + \beta_a\tilde{I}_a + \beta_s\tilde{I}_s)\left[\frac{U + (1-\kappa)V}{U + V + \tilde{\nu}\tilde{a}} - \bar{S}^c\right], \\
&= \tilde{\nu}\tilde{d}\tilde{E} + \tilde{\nu}(\beta_p\tilde{I}_p + \beta_a\tilde{I}_a + \beta_s\tilde{I}_s)\left(\frac{U}{U + V + \tilde{\nu}\tilde{a}} - \frac{\bar{U}^c}{\bar{U}^c + \bar{V}^c}\right) \\
&\quad + \tilde{\nu}(1-\kappa)(\beta_p\tilde{I}_p + \beta_a\tilde{I}_a + \beta_s\tilde{I}_s)\left(\frac{V}{U + V + \tilde{\nu}\tilde{a}} - \frac{\bar{V}^c}{\bar{U}^c + \bar{V}^c}\right) \\
&> 0 \text{ for a sufficiently small } \tilde{\nu} > 0, \\
\dot{I}_p(t) - \frac{\partial(\tilde{\nu}\tilde{I}_p)}{\partial t} &= \theta\tilde{\nu}\tilde{E} - g_p\tilde{\nu}\tilde{I}_p = \tilde{\nu}\tilde{d}\tilde{I}_p > 0, \\
\dot{I}_a(t) - \frac{\partial(\tilde{\nu}\tilde{I}_a)}{\partial t} &= f_a\tilde{\nu}\tilde{I}_p - g_a\tilde{\nu}\tilde{I}_a = \tilde{\nu}\tilde{d}\tilde{I}_a > 0, \\
\dot{I}_s(t) - \frac{\partial(\tilde{\nu}\tilde{I}_s)}{\partial t} &= f_s\tilde{\nu}\tilde{I}_p - g_s\tilde{\nu}\tilde{I}_s = \tilde{\nu}\tilde{d}\tilde{I}_s > 0.
\end{aligned}$$

It appears that $\tilde{\nu}\tilde{\boldsymbol{\Phi}}$ is a sub-solution of $\dot{\boldsymbol{I}} = \boldsymbol{G}(t, \boldsymbol{I})$. Next, we consider the Cauchy problem,

$$\begin{cases} \frac{\partial Q_b(t)}{\partial t} & = & \tilde{\nu}\big(\pi\sigma\tilde{I}_p + \rho_a\tilde{I}_a + \rho_s\tilde{I}_s\big) & - & g_q Q_b(t), & t \geq T, \\ Q_b(T) & = & Q(T), & & & \end{cases}$$

whose solution is a sub-solution of Equation (A3g). We find $\lim_{t\to\infty} Q_b(t) = \underline{Q}$ with $\underline{Q} = \tilde{\nu}\big(\pi\sigma\tilde{I}_p + \rho_a\tilde{I}_a + \rho_s\tilde{I}_s\big)/g_q > 0$. Likewise, we set $\tilde{\underline{Q}} = \min\big\{\underline{Q}, Q(T)\big\}$ and consider the Cauchy problem,

$$\begin{cases} \frac{\partial R_b(t)}{\partial t} & = & \tilde{\nu}\big(\gamma_a\tilde{I}_a + \gamma_s\tilde{I}_s + \gamma_q\tilde{\underline{Q}}\big) & - & g_r R_b, & t \geq T, \\ R_b(T) & = & R(T), & & & \end{cases}$$

Preprints (www.preprints.org) | NOT PEER-REVIEWED | Posted: 5 December 2022 doi:10.20944/preprints202212.0067.v1



whose solution is a sub-solution of Equation (A3h). We find $\lim_{t\to\infty} R_b(t) = \underline{R}$ with $\underline{R} = \tilde{\nu}\big(\gamma_a\tilde{I}_a + \gamma_s\tilde{I}_s + \gamma_q\underline{\tilde{Q}}\big)/g_r > 0$. In a vaccination-dependent situation where $\eta_v > 0$ or $\upsilon > 0$, we have $\tilde{\eta}_v = \eta_v + \upsilon\underline{\tilde{U}} > 0$, and thus $\underline{V} > 0$. This allows picking a $\varrho$ value satisfying

$$0 < \varrho < \min\big\{\underline{U}, \underline{V}, \tilde{\nu}\tilde{E}, \tilde{\nu}\tilde{I}_p, \tilde{\nu}\tilde{I}_a, \tilde{\nu}\tilde{I}_s, \underline{Q}, \underline{R}\big\},$$

so as to obtain $\lim_{t\to\infty} U(t) \geq \varrho$, $\lim_{t\to\infty} V(t) \geq \varrho$, $\lim_{t\to\infty} E(t) \geq \varrho$, $\lim_{t\to\infty} I_p(t) \geq \varrho$, $\lim_{t\to\infty} I_a(t) \geq \varrho$, $\lim_{t\to\infty} I_s(t) \geq \varrho$, $\lim_{t\to\infty} Q(t) \geq \varrho$, and $\lim_{t\to\infty} R(t) \geq \varrho$. When $\eta_v = 0$ and $\upsilon = 0$, Equation (A3b) gives $\dot{V}(t) = -[\alpha + (1-\kappa)\lambda_o(t) + \mu]V(t) \leq -(\alpha+\mu)V(t)$. Any positive solution to $\dot{v}(t) = -(\alpha+\mu)v(t)$, i.e. $v(t) = V_0\mathrm{e}^{-(\alpha+\mu)t}$, is thus a super-solution to Equation (A3b). We here pick a $\varrho$ value satisfying

$$0 < \varrho < \min\big\{\underline{U}, \tilde{\nu}\tilde{E}, \tilde{\nu}\tilde{I}_p, \tilde{\nu}\tilde{I}_a, \tilde{\nu}\tilde{I}_s, \underline{Q}, \underline{R}\big\},$$

as a lower bound for the limits of the state variables, except $\lim_{t\to\infty} V(t) = 0$. □

**Proof of Proposition A3.** The equilibrium point (A10a) follows from setting all the derivatives in System (A3) to zero. Given $\lambda_o$ and $E^\star$, we first solve the system for all other state variables. Indeed, we get Equations (A10e)-(A10i) by solving Equations (A3d)-(A3h) for $I_p$, $I_a$, $I_s$, $Q$ and $R$. We then solve (A3b) for $V$ to obtain Equation (A10c), i.e. $V^\star = \frac{\eta_v + \upsilon U^\star}{g_v + (1-\kappa)\lambda_o}$ where $g_v = \alpha + \mu$. Substituting $V^\star$ for $V$ and the expression (A10i) for $R$ into Equation (A3a), and solving for $U$ leads to Equation (A10b), i.e.

$$U^\star = \frac{[g_v + (1-\kappa)\lambda_o](\eta_u + \epsilon_o e_r E^\star) + \alpha\eta_v}{[g_v + (1-\kappa)\lambda_o](g_u + \lambda_o) - \alpha\upsilon}, \quad \text{and}$$
$$V^\star = \frac{(g_u + \lambda_o)\eta_v + \upsilon(\eta_u + \epsilon_o e_r E^\star)}{[g_v + (1-\kappa)\lambda_o](g_u + \lambda_o) - \alpha\upsilon},$$

where $g_u = \upsilon + \mu$ and $e_r = \theta d_p \sigma d_r$. The next step consists in solving Equation (A3c), i.e.

$$[U^\star + (1-\kappa)V^\star]\lambda_o - g_e E^\star = 0,$$

where $g_e = \theta + \mu$, for $\lambda_o$. To this end, we compute:

$$U^\star + (1-\kappa)V^\star = \frac{[g_v + (1-\kappa)(\upsilon + \lambda_o)](\eta_u + \epsilon_o e_r E^\star) + [\alpha + (1-\kappa)(g_u + \lambda_o)]\eta_v}{[g_v + (1-\kappa)\lambda_o](g_u + \lambda_o) - \alpha\upsilon}.$$

From the definition of $\lambda_o$ in Equation (2), we have $\lambda_o = \frac{\theta d_p[\beta_p + \sigma d_a\beta_a + \sigma d_s\beta_s]E^\star}{N^\star - Q^\star}$ which reads $\lambda_o = \frac{\mathcal{R}_c g_e}{\bar{S}^c}\frac{E^\star}{N^\star - Q^\star}$ from using $\mathcal{R}_c = \frac{\theta d_p}{g_e}[\beta_p + \sigma d_a\beta_a + \sigma d_s\beta_s]\bar{S}^c$, $\bar{S}^c = \frac{U^c + (1-\kappa)V^c}{N^c}$. Summing all the derivatives in System (A3) gives $\dot{N} = \eta - \mu N^\star - \delta_s I_s^\star - \delta_q Q^\star = 0$ from which we obtain

$$N^\star = N^c - \frac{1}{\mu}(\delta_s I_s^\star + \delta_q Q^\star),$$

giving Equation (A10k). We thus have $N^\star - Q^\star = N^c - \theta d_m E^\star$, so that $\lambda_o = \frac{\mathcal{R}_c g_e}{\bar{S}^c}\frac{E^\star}{N^c - \theta d_m E^\star}$. It follows that

$$E^\star = \frac{\bar{S}^c N^c}{\mathcal{R}_c g_e + \bar{S}^c\theta d_m\lambda_o}\lambda_o,$$

resulting in Equation (A10d). Equation (A3c) then reads

$$[U^\star + (1-\kappa)V^\star]\lambda_o - \frac{\bar{S}^c N^c g_e}{\mathcal{R}_c g_e + \bar{S}^c\theta d_m\lambda_o}\lambda_o = 0.$$

 doi:10.20944/preprints202212.0067.v1



The obvious solution $\lambda_o = 0$ corresponds to the d.f.e., and we here consider $\lambda_o > 0$ as implied by the presence of disease. Hence we have

$$\frac{[g_v + (1-\kappa)(\upsilon + \lambda_o)](\eta_u + \epsilon_o e_r E^\star) + [\alpha + (1-\kappa)(g_u + \lambda_o)]\eta_v}{[g_v + (1-\kappa)\lambda_o](g_u + \lambda_o) - \alpha\upsilon} - \frac{\bar{S}^c N^c g_e}{\mathcal{R}_c g_e + \bar{S}^c \theta d_m \lambda_o} = 0.$$

Using the identity $\eta_u[g_v + (1-\kappa)\upsilon] + \eta_v[\alpha + (1-\kappa)g_u] = \bar{S}^c N^c(g_u g_v - \alpha\upsilon)$ and setting $L_1 = \bar{S}^c N^c\big[\theta[d_m\mu + d_p\sigma d_r\epsilon_o]g_{uv} - \kappa p_v \theta d_m \mu^2 + (1-\kappa)\theta d_p \mu\beta_\sigma - (\theta+\mu)[g_{uv} + (1-\kappa)\mu]\big]$, and $L_2 = (1-\kappa)\bar{S}^c N^c[\theta(d_m\mu + d_p\sigma d_r\epsilon_o) - (\theta+\mu)]$ with $g_{uv} = \alpha + (1-\kappa)\upsilon + \mu$, and $\beta_\sigma = \beta_p + \sigma d_a\beta_a + \sigma d_s\beta_s$, we get the quadratic equation

$$L_2\lambda_o^2 + L_1\lambda_o + \bar{S}^c N^c g_e(g_u g_v - \alpha\upsilon)(\mathcal{R}_c - 1) = 0,$$

Note that the definitions of $d_p$, $d_m$, and $d_r$ imply that:

$$\begin{aligned} d_m\mu + d_p\sigma d_r\epsilon_o = d_p\sigma\left[d_a\gamma_a\frac{\epsilon_o}{\epsilon_o+\mu} + d_s\left(\delta_s + \gamma_s\frac{\epsilon_o}{\epsilon_o+\mu}\right) + d_q\left(\mu + \delta_q + \gamma_q\frac{\epsilon_o}{\epsilon_o+\mu}\right)\right], \\ < d_p\sigma[d_a\gamma_a + d_s(\delta_s+\gamma_s) + d_q(\mu + \delta_q + \gamma_q)], \\ < d_p\sigma[d_a(\gamma_a + \rho_a) + d_s(\delta_s + \gamma_s + \rho_s) + \pi], \\ < d_p\sigma[(1-\tau)(1-\pi) + \tau(1-\pi) + \pi], \\ < d_p\sigma, \\ < 1. \end{aligned}$$

It follows that $L_2 < 0$. For $\mathcal{R}_c \leq 1$, on using $\bar{S}^c \geq 1 - \kappa$, we have $(1-\kappa)\theta d_p\beta_\sigma \leq g_e$ which implies that $L_1 \leq 0$, and since $(g_u g_v - \alpha\upsilon) = \mu(\alpha + \upsilon + \mu) > 0$, the constant term $L_0 = \bar{S}^c N^c g_e(g_u g_v - \alpha\upsilon)(\mathcal{R}_c - 1)$ also satisfies $L_0 \leq 0$. Therefore, the above quadratic equation in $\lambda_o$ has no positive solution when $\mathcal{R}_c \leq 1$. As a result, a positive endemic equilibrium exists only if $\mathcal{R}_c > 1$. Since $L_0 > 0$ when $\mathcal{R}_c > 1$, the quadratic then has a unique positive root $\lambda_o^\star$ given by

$$\lambda_o^\star = \frac{1}{2}\left(-K_1 + \sqrt{K_1^2 + 4K_0}\right)$$

where $K_0 = -L_0/L_2$ and $K_1 = L_1/L_2$. □

**Proof of Lemma A4.** Let $\bar{U}^\star = \frac{U^\star}{N^\star - Q^\star}$, $\bar{V}^\star = \frac{V^\star}{N^\star - Q^\star}$, $\bar{V}_\kappa^\star = (1-\kappa)\bar{V}^\star$, $\bar{S}^\star = \bar{U}^\star + \bar{V}_\kappa^\star$, $\upsilon^\star = \upsilon + \bar{V}_\kappa^\star\lambda_o^\star$, $\alpha^\star = \alpha + \bar{U}^\star\lambda_o^\star$, $\epsilon_o^\star = \epsilon_o + \bar{U}^\star\lambda_o^\star$, $h_u^\star = 1 - \bar{S}^\star$, $h_v^\star = 1 - \kappa - \bar{S}^\star$, $g_u^\star = \upsilon + \mu + (1-\bar{U}^\star)\lambda_o^\star$, $g_v^\star = \alpha + \mu + (1-\kappa)(1-\bar{V})\lambda_o^\star$, $g_e^\star = \theta + \mu + \bar{S}^\star\lambda_o^\star$, and $g_r = \epsilon_o + \mu$. Then, the Jacobian matrix $\boldsymbol{J}^\star$ of the UVEIQR model (A3) evaluated at the endemic equilibrium (e.e.) point $\boldsymbol{X}^\star$ has the block structure

$$\boldsymbol{J}^\star = \begin{pmatrix} \boldsymbol{J}_{11}^\star & \boldsymbol{J}_{12}^\star \\ \boldsymbol{J}_{21}^\star & \boldsymbol{J}_{22}^\star \end{pmatrix},\ \boldsymbol{J}_{11}^\star = \begin{pmatrix} -g_u^\star & \alpha^\star & \bar{U}^\star\lambda_o^\star \\ \upsilon^\star & -g_v^\star & \bar{V}_\kappa^\star\lambda_o^\star \\ h_u^\star\lambda_o^\star & h_v^\star\lambda_o^\star & -g_e^\star \end{pmatrix},\ \boldsymbol{J}_{22}^\star = \begin{pmatrix} -g_p & 0 & 0 & 0 & 0 \\ f_a & -g_a & 0 & 0 & 0 \\ f_s & 0 & -g_s & 0 & 0 \\ \pi\sigma & \rho_a & \rho_s & -g_q & 0 \\ 0 & \gamma_a & \gamma_s & \gamma_q & -g_r \end{pmatrix},$$

$$\boldsymbol{J}_{21}^\star = \begin{pmatrix} 0 & 0 & \theta \\ 0 & 0 & 0 \\ 0 & 0 & 0 \\ 0 & 0 & 0 \\ 0 & 0 & 0 \end{pmatrix} \text{ and } \boldsymbol{J}_{12}^\star = \begin{pmatrix} \bar{U}^\star(\lambda_o^\star - \beta_p) & \bar{U}^\star(\lambda_o^\star - \beta_a) & \bar{U}^\star(\lambda_o^\star - \beta_s) & 0 & \epsilon_o^\star \\ \bar{V}_\kappa^\star(\lambda_o^\star - \beta_p) & \bar{V}_\kappa^\star(\lambda_o^\star - \beta_a) & \bar{V}_\kappa^\star(\lambda_o^\star - \beta_s) & 0 & \bar{V}_\kappa^\star\lambda_o^\star \\ \bar{S}^\star(\beta_p - \lambda_o^\star) & \bar{S}^\star(\beta_a - \lambda_o^\star) & \bar{S}^\star(\beta_s - \lambda_o^\star) & 0 & -\bar{S}^\star\lambda_o^\star \end{pmatrix}.$$

Let $k$ be an arbitrary complex number and $\boldsymbol{Z} = (z_1, \cdots, z_8)^\top$ be a nonzero complex vector. To establish l.a.s. for the e.e. point $\boldsymbol{X}^\star$, we use Krasnoselskii [84]'s sublinearity trick, a technique described for stability analysis in Hethcote and Thieme [85], to show that any

solution of the form $\boldsymbol{Z}_0 = \boldsymbol{Z}e^{kt}$ for System (A3) linearized around $\boldsymbol{X}^\star$ (i.e. $\dot{\boldsymbol{X}} = \boldsymbol{J}^\star\boldsymbol{X}$) satisfies $Re(k) < 0$. Substituting $\boldsymbol{Z}_0$ into the linear system results in $k\boldsymbol{Z} = \boldsymbol{J}^\star\boldsymbol{Z}$. Following Hethcote and Thieme [85], we use contradiction to show that $Re(k) < 0$ for any $\boldsymbol{Z}$ solution of $k\boldsymbol{Z} = \boldsymbol{J}^\star\boldsymbol{Z}$.

First assume that $k = 0$. Then $\boldsymbol{J}^\star\boldsymbol{Z} = \boldsymbol{0}$ and the system has a nonzero solution $\boldsymbol{Z}$ only if $\det(\boldsymbol{J}^\star) = 0$. From the block structure of $\boldsymbol{J}^\star$, we have $\det(\boldsymbol{J}^\star) = \det(\boldsymbol{J}_{22}) \times \det(\boldsymbol{C}_\star)$ where $\boldsymbol{C}_\star$ is the Schur complement of $\boldsymbol{J}^\star_{22}$ in $\boldsymbol{J}^\star$: $\boldsymbol{C}_\star = \boldsymbol{J}^\star_{11} - \boldsymbol{J}^\star_{12}[\boldsymbol{J}^\star_{22}]^{-1}\boldsymbol{J}^\star_{21}$. We obtain $\det(\boldsymbol{J}_{22}) = -g_p g_a g_s g_q g_r$ and

$$\boldsymbol{C}_\star = \begin{pmatrix} -g_u^\star & \alpha^\star & \bar{U}^\star\lambda_o^\star - g_p^{-1}\theta\big(\bar{U}^\star y_0^\star + f_r(0)g_r^{-1}\epsilon_o\big) \\ \upsilon^\star & -g_v^\star & \bar{V}_\kappa^\star\lambda_o^\star - g_p^{-1}\theta\bar{V}_\kappa^\star y_0^\star \\ h_u^\star\lambda_o^\star & h_v^\star\lambda_o^\star & -g_e^\star + g_p^{-1}\theta\bar{S}^\star y_0^\star \end{pmatrix}$$

where we have set $y_0^\star = \lambda_o^\star\big(1 + f_a g_a^{-1} + f_s g_s^{-1} + f_r(0)g_r^{-1}\big) - \big(\beta_p + f_a g_a^{-1}\beta_a + f_s g_s^{-1}\beta_s\big)$, and $f_r(k) = \frac{\pi\sigma}{k+g_q}\gamma_q + \frac{f_a}{k+g_a}\Big(\gamma_a + \frac{\rho_a\gamma_q}{k+g_q}\Big) + \frac{f_s}{k+g_s}\Big(\gamma_s + \frac{\rho_s\gamma_q}{k+g_q}\Big)$. It turns out that

$$\begin{aligned}\det(\boldsymbol{C}_\star) = {} & (g_u^\star g_v^\star - \alpha^\star\upsilon^\star)\big(g_p^{-1}\theta\bar{S}^\star y_0^\star - g_e^\star\big) - \theta g_p^{-1} f_r(0) g_r^{-1}\lambda_o^\star(h_v^\star\upsilon^\star + h_u^\star g_v^\star)\epsilon_o \\ & + [(h_v^\star\upsilon^\star + h_u^\star g_v^\star)\bar{U}^\star + (h_u^\star\alpha^\star + h_v^\star g_u^\star)\bar{V}_\kappa^\star]\lambda_o^\star\big(\lambda_o^\star - \theta g_p^{-1}y_0^\star\big),\end{aligned}$$

hence $\det(\boldsymbol{C}_\star) < 0$ and $\det(\boldsymbol{J}^\star) > 0$. Therefore $k \neq 0$. Next, assume that $Re(k) > 0$. The Eigen equation $k\boldsymbol{Z} = \boldsymbol{J}^\star\boldsymbol{Z}$ reads

$$\begin{aligned}
kz_1 &= -g_u^\star z_1 + \alpha^\star z_2 + \bar{U}^\star\lambda_o^\star z_3 + \bar{U}^\star(\lambda_o^\star - \beta_p)z_4 + \bar{U}^\star(\lambda_o^\star - \beta_a)z_5 + \bar{U}^\star(\lambda_o^\star - \beta_s)z_6 + \epsilon_o^\star z_8, \\
kz_2 &= \upsilon^\star z_1 - g_v^\star z_2 + \bar{V}_\kappa^\star\lambda_o^\star z_3 + \bar{V}_\kappa^\star(\lambda_o^\star - \beta_p)z_4 + \bar{V}_\kappa^\star(\lambda_o^\star - \beta_a)z_5 + \bar{V}_\kappa^\star(\lambda_o^\star - \beta_s)z_6 + \bar{V}_\kappa^\star\lambda_o^\star z_8, \\
kz_3 &= h_u^\star\lambda_o^\star z_1 + h_v^\star\lambda_o^\star z_2 - g_e^\star z_3 + \bar{S}^\star(\beta_p - \lambda_o^\star)z_4 + \bar{S}^\star(\beta_a - \lambda_o^\star)z_5 + \bar{S}^\star(\beta_s - \lambda_o^\star)z_6 - \bar{S}^\star\lambda_o^\star z_8, \\
kz_4 &= \theta z_3 - g_p z_4, \\
kz_5 &= f_a z_4 - g_a z_5, \\
kz_6 &= f_s z_4 - g_s z_6, \\
kz_7 &= \pi\sigma z_4 + \rho_a z_5 + \rho_s z_6 - g_q z_7, \\
kz_8 &= \gamma_a z_5 + \gamma_s z_6 + \gamma_q z_7 - g_r z_8.
\end{aligned}$$

Subsequently solving the last five equations of the previous system for $z_j$ $(j = 4, \cdots, 8)$ leads to $z_8 = \theta(k+g_p)^{-1}f_r(k)(k+g_r)^{-1}z_3$. Then, setting $z_m = z_8 + \sum_{j=1}^{6} z_j$, and rearranging the first three equations yields:

$$(k + g_u + \lambda_o^\star)z_1 = \alpha z_2 + \bar{U}^\star\lambda_o^\star z_m - \bar{U}^\star(\beta_p z_4 + \beta_a z_5 + \beta_s z_6) + \epsilon_o z_8, \tag{A13}$$

$$[k + g_v + (1-\kappa)\lambda_o^\star]z_2 = \upsilon z_1 + \bar{V}_\kappa^\star\lambda_o^\star z_m - \bar{V}_\kappa^\star(\beta_p z_4 + \beta_a z_5 + \beta_s z_6), \tag{A14}$$

$$(k + g_e)z_3 = \lambda_o^\star[z_1 + (1-\kappa)z_2] - \bar{S}^\star\lambda_o^\star z_m + \bar{S}^\star(\beta_p z_4 + \beta_a z_5 + \beta_s z_6). \tag{A15}$$

Summing Equations (A13)-(A15) leads after some additional algebra to

$$(k+\mu)(z_1 + z_2) = -(k + \mu + \theta)z_3 + \epsilon_o(k+g_p)^{-1}f_r(k)(k+g_r)^{-1}\theta z_3, \tag{A16}$$

$$\begin{aligned}
z_m = {} & (k+g_p)^{-1}\left(1 + \frac{f_a}{k+g_a} + \frac{f_s}{k+g_s} + \frac{f_r(k)}{k+g_r}\right)\theta z_3 \\
& - (k+\mu)^{-1}\left[1 - \frac{\epsilon_o f_r(k)}{(k+g_p)(k+g_r)}\right]\theta z_3, \quad \text{and} \\
[z_1 + (1-\kappa)z_2] = {} & \bar{S}^\star z_m + \frac{\kappa(1-\kappa)\bar{V}^\star}{k+g_{uv}^\star}(\beta_p z_4 + \beta_a z_5 + \beta_s z_6) - \left(1 - \frac{\kappa\upsilon}{k+g_{uv}^\star}\right)z_3 \\
& - \left[1 - \frac{\epsilon_o f_r(k)}{(k+g_p)(k+g_r)}\right]\left[1 - \frac{\kappa[\upsilon + (1-\kappa)\bar{V}^\star]}{k+g_{uv}^\star} - \bar{S}^\star\right]\frac{\theta}{k+\mu}z_3 \\
& - \bar{S}^\star\left(1 + \frac{f_a}{k+g_a} + \frac{f_s}{k+g_s} + \frac{f_r(k)}{k+g_r}\right)\frac{\theta}{k+g_p}z_3,
\end{aligned}$$

Preprints (www.preprints.org) | NOT PEER-REVIEWED | Posted: 5 December 2022 doi:10.20944/preprints202212.0067.v1



where $g^\star_{uv} = \alpha + \upsilon + \mu + (1-\kappa)\lambda^\star_o$. Equation (A15) then becomes:

$$
\begin{aligned}
[g_e + k + a_3(k)]z_3 &= \left[\bar{S}^\star + \frac{\kappa\bar{V}^\star(1-\kappa)\lambda^\star_o}{k+g^\star_{uv}}\right](\beta_p z_4 + \beta_a z_5 + \beta_s z6) \quad \text{where} \\
a_3(k) &= \left[1 - \frac{\epsilon_o f_r(k)}{(k+g_p)(k+g_r)}\right]\left[1 - \frac{\kappa[\upsilon + (1-\kappa)\bar{V}^\star]}{k+g^\star_{uv}} - \bar{S}^\star\right]\frac{\lambda^\star_o\theta}{k+\mu} \\
&\quad + \left(1 + \frac{f_a}{k+g_a} + \frac{f_s}{k+g_s} + \frac{f_r(k)}{k+g_r}\right)\frac{\bar{S}^\star\lambda^\star_o\theta}{k+g_p} + \left(1 - \frac{\kappa\upsilon}{k+g^\star_{uv}}\right)\lambda^\star_o.
\end{aligned}
$$

On defining $\overline{\boldsymbol{Z}} = (z_3, \cdots, z_8)^\top$, we obtain the system

$$
[b_j + F_j(k)](\overline{\boldsymbol{Z}})_{j-2} = \left(\boldsymbol{H}\overline{\boldsymbol{Z}}\right)_{j-2} \quad \text{for} \quad j = 3, 4, \cdots, 8,
$$

where we have set $F_3(k) = g_e^{-1}b_3[k + a_3(k)]$, $F_4(k) = g_p^{-1}k$, $F_5(k) = g_a^{-1}k$, $F_6(k) = g_s^{-1}k$, $F_7(k) = g_q^{-1}k$, $F_8(k) = g_r^{-1}k$, $b_3 = \bar{S}^\star\left[\bar{S}^\star + \frac{\kappa\bar{V}^\star(1-\kappa)\lambda^\star_o}{k+g^\star_{uv}}\right]^{-1}$, $b_j = 1$ for $j = 4, \cdots, 8$, and

$$
\boldsymbol{H} = \begin{pmatrix}
0 & g_e^{-1}\bar{S}^\star\beta_p & g_e^{-1}\bar{S}^\star\beta_a & g_e^{-1}\bar{S}^\star\beta_s & 0 & 0 \\
g_p^{-1}\theta & 0 & 0 & 0 & 0 & 0 \\
0 & g_a^{-1}f_a & 0 & 0 & 0 & 0 \\
0 & g_s^{-1}f_s & 0 & 0 & 0 & 0 \\
0 & g_q^{-1}\pi\sigma & g_q^{-1}\rho_a & g_q^{-1}\rho_s & 0 & 0 \\
0 & 0 & g_r^{-1}\gamma_a & g_r^{-1}\gamma_s & g_r^{-1}\gamma_q & 0
\end{pmatrix}.
$$

Note that the matrix $\boldsymbol{H}$ is nonnegative and satisfies $\boldsymbol{H}\boldsymbol{E}^\star = \boldsymbol{E}^\star$ where $\boldsymbol{E}^\star$ contains the endemic sizes of infected classes, i.e. $\boldsymbol{E}^\star = \left(E^\star, I_p^\star, I_a^\star, I_s^\star, Q^\star, R^\star\right)^\top$. Taking norms elementwise and setting $F(k) = \inf\left\{Re(F_j(k)), j = 3, \cdots, 8\right\}$ and $b_0 = Re(b_3)$, we get

$$
[b_0 + F(k)]|\overline{\boldsymbol{Z}}| \leq \boldsymbol{H}|\overline{\boldsymbol{Z}}| \tag{A17}
$$

where $|\overline{\boldsymbol{Z}}| = (|z_3|, \cdots, |z_8|)^\top$. It appears that $Re(a_3(k)) > 0$ and $b_0 \in (0, 1]$ for $Re(k) > 0$. Therefore, $Re(F_j(k)) > 0$ for all $j = 3, \cdots, 8$, hence $F(k) > 0$. Let $r_0$ denote the minimum number such that $|\overline{\boldsymbol{Z}}| \leq r_0 b_0 \boldsymbol{E}^\star$. The positivity of $b_0\boldsymbol{E}^\star$ ensures that $r_0$ is positive and finite, and $r = r_0 b_0$ is the minimum number such that $|\overline{\boldsymbol{Z}}| \leq r\boldsymbol{E}^\star$. The inequality (A17) then implies that $[b_0 + F(k)]|\overline{\boldsymbol{Z}}| \leq \boldsymbol{H}|\overline{\boldsymbol{Z}}| \leq r\boldsymbol{H}\boldsymbol{E}^\star = r_0 b_0 \boldsymbol{E}^\star$ which leads to $|\overline{\boldsymbol{Z}}| \leq \frac{r_0 b_0}{b_0 + F(k)}\boldsymbol{E}^\star$. From $b_0 > 0$ and $F(k) > 0$, we have $\frac{b_0}{b_0+F(k)} < b_0$, hence $|\overline{\boldsymbol{Z}}| \leq \frac{r_0 b_0}{b_0+F(k)}\boldsymbol{E}^\star < r\boldsymbol{E}^\star$ contradicts the minimality of $r$. Therefore, $Re(k) < 0$ (i.e. all eigenvalues of $\boldsymbol{J}^\star$ have negative real parts) and l.a.s. is established for $\boldsymbol{X}^\star$. □

**Proof of Proposition A4.** Let $\boldsymbol{X} = (U, V, E, I_p, I_a, I_s, Q, R)^\top$ be the vector of the states of the model (A3). For simplicity, we relabel the state variables $x_j$ $(j = 1, 2, \cdots, 8)$ such that $\boldsymbol{X} = (x_1, x_2, \cdots, x_8)^\top$. Let us define the function $L$ given for $t \geq 0$ by

$$
L(t) = \sum_{j=1}^{8}\left(x_j - x_j^\star \log x_j\right).
$$

We claim that $L$ is a strict Lyapunov function [86] as we next show. It first appears that $L$ is continuous everywhere and has first order partial derivatives with respect to $\boldsymbol{X}$ (i.e. system (A3)). Thus, we are only required to show that the first derivative $\dot{L}$ of $L$ with respect to time satisfies $\dot{L}(t) \leq 0$ for any solution $\boldsymbol{X}$ as $t \to \infty$. To this end, we have

$$
\dot{L}(t) = \sum_{j=1}^{8}\left(x_j - x_j^\star\right)\frac{\dot{x}_j}{x_j}.
$$

Preprints (www.preprints.org) | NOT PEER-REVIEWED | Posted: 5 December 2022 doi:10.20944/preprints202212.0067.v1



Note that $\dot{L}(t) = 0$ for $\boldsymbol{X} = \boldsymbol{X}^\star$. By Lemma (A3), each $x_j$ is bounded and there exists $\underline{x} = \min x_j$ such that $\underline{x} > 0$ as $t \to \infty$ (in the vaccination-free context where $\eta_v = \upsilon = 0$, the same argument holds by ignoring the state $V$ which satisfies $V(t) \to V^\star = 0$ as $t \to \infty$). This implies that

$$\dot{L}(t) \leq \underline{x}^{-1} \sum_{j=1}^{8} (x_j - x_j^\star)\dot{x}_j.$$

Since the derivatives $\dot{x}_j$ in system (A3) are additive functions of constant parameters and bounded variables $x_j$, it also follows that each $\dot{x}_j$ is bounded so that there exists $\overline{x} > 0$ such that $\dot{x}_j < \overline{x}$ for $j = 1, 2, \cdots, 8$. This implies that

$$\dot{L}(t) < \overline{x}\underline{x}^{-1} \sum_{j=1}^{8} (x_j - x_j^\star) \quad \text{for} \quad \boldsymbol{X} \neq \boldsymbol{X}^\star.$$

Since $N$ is bounded, it follows from Barbalat's lemma [87] that $\dot{N}(t) \to 0$ as $t \to \infty$, so that we have from $\dot{N}(t) = \eta - \mu N(t) - \delta_s I_s(t) - \delta_q Q(t)$:

$$\lim_{t\to\infty} N(t) = N^c - \frac{1}{\mu} \lim_{t\to\infty} [\delta_s I_s(t) + \delta_q Q(t)].$$

We also have $\lim_{t\to\infty} \dot{I}_s(t) = \lim_{t\to\infty} \dot{Q}(t) = 0$ by Barbalat's lemma and the boundedness of $I_s(t)$ and $Q(t)$, so that $\lim_{t\to\infty} I_s(t)$ and $\lim_{t\to\infty} Q(t)$ are stationary points for Equations (A3f) and (A3g). Since these limits are nonzero when $\mathcal{R}_c > 1$ (by Lemma (A3)), the d.f.e. ($I_s^c = 0$ and $Q^c = 0$) is excluded, and $\lim_{t\to\infty} I_s(t) = I_s^\star$ and $\lim_{t\to\infty} Q(t) = Q^\star$ (the unique e.e. alternative). It follows, by Equation (A10k), that $\lim_{t\to\infty} N(t) = N^\star$, so that $\lim_{t\to\infty} \sum_{j=1}^{8} \left(x_j - x_j^\star\right) = \lim_{t\to\infty} N(t) - N^\star = 0$. As a result, $\dot{L}(t) < 0$ for $\boldsymbol{X} \neq \boldsymbol{X}^\star$ as $t \to \infty$, hence $L$ is a strict Lyapunov function, and by Proposition (A3), $\boldsymbol{X}^\star$ is its unique stationary point: $\boldsymbol{X}^\star$ is a global minimum and therefore g.a.s. when $\mathcal{R}_c > 1$. □

*Appendix C.2. Proofs of Lemmas and Propositions Related to Disease-Opinion Dynamics*

**Proof of Lemma 1.** A proof of Lemma 1 is straightforward following the argument detailled in the proof of Lemma A1 (see Appendix C.1). Each compartment size $x_j(t)$ satisfies $\frac{\partial x_j(t)}{\partial t} \geq -z_{0j} x_j(t)$ where $z_{0j}$ is a positive real constant. This gives $x_j(t) \geq x_{0j} e^{-z_{0j} t}$, which establishes nonnegativity from $x_{0j} \geq 0$. This implies that the total population size $N(t) = \sum_j x_j(t)$ satisfies $N(t) \geq 0$. Then, $\frac{\partial N(t)}{\partial t} \leq \eta - \mu N(t)$ leads to $0 \leq N(t) \leq \max\{N_0, N^c\}$ where $N^c = \eta/\mu$ is the carrying capacity of the biological system. This finally results in $0 \leq x_j(t) \leq \max\{N_0, N^c\}$. □

**Proof of Proposition 1.** Adding the disease-free restriction $E = I_p = I_a = I_s = Q = 0$ to System (7) implies that $\lambda_i(t) = 0$. Setting all the derivatives to zero then gives $E^c = I_p^c = I_a^c = I_s^c = Q^c = R^c = 0$. Since $w_o > 0$, we are left with the system

$$\begin{aligned} \bar{\eta}_1 - S_{-1}^c S_1^c - \bar{\mu} S_1^c &= 0, \\ \bar{\eta}_0 + 2S_{-1}^c S_1^c - \bar{\mu} S_0^c &= 0, \\ \bar{\eta}_{-1} - S_1^c S_{-1}^c - \bar{\mu} S_{-1}^c &= 0, \end{aligned}$$

where $\bar{\eta}_i = \eta_i \frac{N^c}{w_o}$, $\bar{\mu} = \mu \frac{N^c}{w_o}$ with $N^c = S_{-1}^c + S_0^c + S_1^c$. Summing the three equations gives $\eta - \mu N^c = 0$, i.e. $N^c = \eta/\mu$. Solving the third equation for $S_{-1}^c$ gives $S_{-1}^c = \frac{\bar{\eta}_{-1}}{S_1^c + \bar{\mu}}$, and inserting this in the first equation yields the quadratic $\bar{\mu}(S_1^c)^2 - \left(\bar{\eta}_1 - \bar{\eta}_{-1} - \bar{\mu}^2\right) S_1^c - \bar{\eta}_1 \bar{\mu}$ which has the unique positive solution

$$S_1^c = \frac{1}{2\bar{\mu}} \left[ \sqrt{\left(\bar{\eta}_1 - \bar{\eta}_{-1} - \bar{\mu}^2\right)^2 + 4\bar{\eta}_1 \bar{\mu}^2} + \bar{\eta}_1 - \bar{\eta}_{-1} - \bar{\mu}^2 \right].$$

Preprints (www.preprints.org) | NOT PEER-REVIEWED | Posted: 5 December 2022 doi:10.20944/preprints202212.0067.v1



Further simplifications yield Equation (25c), and Equations (25a) and (25b) follow. The computations of the reproduction numbers (16a) and (16b) follow the steps in the proof of Proposition A1 (see Appendix C.1), except that $\mathbb{F}(\boldsymbol{I})$ and $\boldsymbol{F}^c$ are here defined as

$$\mathbb{F}(\boldsymbol{I}) = \frac{1}{N-Q}\sum_{i\in\mathcal{P}} S_i \begin{pmatrix} \sum_{j=p,a,s}\beta_{ij}I_j \\ 0 \\ 0 \\ 0 \end{pmatrix} \text{ and } \boldsymbol{F}^c = \frac{1}{N^c}\sum_{i=-1}^{1} S_i^c \begin{pmatrix} 0 & \beta_{ip} & \beta_{ia} & \beta_{is} \\ 0 & 0 & 0 & 0 \\ 0 & 0 & 0 & 0 \\ 0 & 0 & 0 & 0 \end{pmatrix}.$$

To obtain the direction of variation of the basic reproduction number $\mathcal{R}_0$ (16a) as a function of the baseline influence rate $w_o$, we find its derivative with respect to $w_o$. To this end, the derivatives of $S^c_{-1}$ and $S^c_1$ with respect to $w_o$ are the same as we next explain. First, we obtain after basic algebra $\frac{\partial S^c_1}{\partial w_o} = \frac{\eta}{2w_o}\left[1 - \frac{(\mu+w_o)\eta - w_o\eta_0}{2w_o\mu\sqrt{\Delta_1}}\right] < 0$ where we have set $\Delta_1 = \frac{\eta\eta_1}{\mu w_o} + \left(\frac{\eta_1-\eta_{-1}}{2\mu} - \frac{\eta}{2w_o}\right)^2$. We next notice that $S^c_{-1}$ is given by Equation (25c) on switching the roles of $\eta_{-1}$ and $\eta_1$. It then follows that $\frac{\partial S^c_{-1}}{\partial w_o} = \frac{\eta}{2w_o}\left[1 - \frac{(\mu+w_o)\eta - w_o\eta_0}{2w_o\mu\sqrt{\Delta_{-1}}}\right] < 0$ with $\Delta_{-1} = \frac{\eta\eta_{-1}}{\mu w_o} + \left(\frac{\eta_{-1}-\eta_1}{2\mu} - \frac{\eta}{2w_o}\right)^2$. Writing $\Delta_1 = \frac{\eta(\eta_{-1}+\eta_1)}{2\mu w_o} + \left(\frac{\eta_1-\eta_{-1}}{2\mu}\right)^2 + \left(\frac{\eta}{2w_o}\right)^2$ finally shows that $\Delta_1 = \Delta_{-1}$ hence $\frac{\partial S^c_{-1}}{\partial w_o} = \frac{\partial S^c_1}{\partial w_o}$. This implies that $\frac{\partial S^c_0}{\partial w_o} = -2\frac{\partial S^c_{-1}}{\partial w_o}$ and $\frac{\partial \mathcal{R}_0}{\partial w_o} = \mathcal{R}_{00}\left(\varsigma_o^2 - 2\varsigma_o + 1\right)\frac{\partial S^c_1}{\partial w_o} < 0$ with $\mathcal{R}_{00} = \frac{\theta}{(\theta+\mu)(\sigma+\mu)}\frac{\mu}{\eta}\sum_{j=p,a,s}\beta_j m_j$. □

**Proof of Proposition 2.** Adding the disease-free restriction $E = I_p = I_a = I_s = Q = 0$ to System (14) implies that $\lambda_i(t) = 0$. Setting all the derivatives to zero then gives $E^c = I^c_p = I^c_a = I^c_s = Q^c = R^c = 0$ and we are left with the system

$$\boldsymbol{M}\boldsymbol{S}^c = \boldsymbol{\eta}$$

where $\boldsymbol{S}^c$, $\boldsymbol{M}$, and $\boldsymbol{\eta}$ are as defined in Equation (19b). Summing the partial derivatives for all $S_i$ individuals gives $\dot{U}_{iu} + \dot{U}_{iv} + \dot{V}_i = \dot{S}_i$, i.e. the susceptible states in the SEIQR-Opinion model (7). It follows that $S^c_1$, $S^c_{-1}$, and $S^c_0$ are given by Equations (25c)–(25b). Likewise, summing the first three equations, the fourth to sixth equations, and the seventh to last equations results in the system

$$\begin{array}{rcrcrcrcrcrcl}
\bar{\eta}_{uu} & + & U^c_u U^c_v & - & (U^c_v + V^c)U^c_u & & & & & - & \bar{\mu}U^c_u = 0 & (a), \\
\bar{\eta}_{uv} & - & U^c_u U^c_v & + & (U^c_v + V^c)U^c_u & + & \bar{\alpha}V^c & - & \bar{\upsilon}U_v & - & \bar{\mu}U^c_v = 0 & (b), \\
\bar{\eta}_v & & & & & - & \bar{\alpha}V^c & + & \bar{\upsilon}U_v & - & \bar{\mu}V^c = 0 & (c),
\end{array}$$

where $\bar{\eta}_{uu} = \sum_{i\in\mathcal{P}}\bar{\eta}_{iu}$, $\bar{\eta}_{uv} = \sum_{i\in\mathcal{P}}\bar{\eta}_{iuv}$, $\bar{\eta}_v = \sum_{i\in\mathcal{P}}\bar{\eta}_{iv}$, $\bar{\eta}_{il} = \eta_{il}\frac{N^c}{w_o}$, $\bar{\mu} = \mu\frac{N^c}{w_o}$, $\bar{\alpha} = \alpha\frac{N^c}{w_o}$, $\bar{\upsilon} = \upsilon\frac{N^c}{w_o}$, $U^c_u = \sum_{i\in\mathcal{P}}U^c_{iu}$, $U^c_v = \sum_{i\in\mathcal{P}}U^c_{iv}$, and $V^c = \sum_{i\in\mathcal{P}}V^c_i$. From $(c)$, we have $V^c = \frac{\bar{\eta}^c_v + \bar{\upsilon}U_v}{\bar{\alpha}+\bar{\mu}}$, and from $(a)$ we get $U^c_u = \frac{\bar{\eta}_{uu}}{V^c+\bar{\mu}} = \frac{\bar{\eta}_{uu}(\bar{\alpha}+\bar{\mu})}{\bar{\eta}_v + \bar{\mu}(\bar{\alpha}+\bar{\mu}) + \bar{\upsilon}U^c_v}$. Inserting these results in $(b)$ leads to the quadratic $A(U^c_v)^2 + BU^c_v - C = 0$ where $A = \upsilon\left(1 + \frac{\upsilon}{\alpha+\mu}\right)$, $B = \eta_u\left(\frac{\alpha+\upsilon+\mu}{w_o} - \frac{\upsilon}{\mu}\right) + \eta_v\left(1 + \frac{\alpha+\upsilon+\mu}{w_o} + \frac{\upsilon(\mu-\alpha)}{\mu(\alpha+\mu)}\right)$, $C = \eta\eta_{uv}\frac{\alpha+\mu}{w_o\mu} + \frac{\eta_v}{\mu}\left(\eta_u + \frac{\alpha\eta_v}{\alpha+\mu} + \frac{\alpha\eta}{w_o}\right)$. We thus have the constants $U^c_u$, $U^c_v$ and $V^c$, and in consequence, the matrix $\boldsymbol{M}$. It follows that $\boldsymbol{M}\boldsymbol{S}^c = \boldsymbol{\eta}$ is a linear system in $\boldsymbol{S}^c$. The step-wise resolution of the system $\boldsymbol{M}\boldsymbol{S}^c = \boldsymbol{\eta}$ in Appendix D proves that the matrix $\boldsymbol{M}$ is non-singular, and Equation (19b) follows. The computations of the reproduction numbers (20a) and (20c) follow the steps in the

 doi:10.20944/preprints202212.0067.v1



proof of Proposition A1 (see Appendix C.1), except that $\mathbb{F}(\boldsymbol{I})$ and $\boldsymbol{F}^c$ are defined with $\bar{S}_i = \frac{U_i+(1-\kappa)V_i}{N-Q}$ and $\bar{S}_i^c = \frac{U_i^c+(1-\kappa)V_i^c}{N^c}$ as

$$\mathbb{F}(\boldsymbol{I}) = \sum_{i\in\mathcal{P}} \bar{S}_i \begin{pmatrix} \sum_{j=p,a,s} \beta_{ij} I_j \\ 0 \\ 0 \\ 0 \end{pmatrix} \text{ and } \boldsymbol{F}^c = \sum_{i\in\mathcal{P}} \bar{S}_i^c \begin{pmatrix} 0 & \beta_{ip} & \beta_{ia} & \beta_{is} \\ 0 & 0 & 0 & 0 \\ 0 & 0 & 0 & 0 \\ 0 & 0 & 0 & 0 \end{pmatrix}.$$

The derivatives of $g_i(\boldsymbol{M}) = U_i^c + (1-\kappa)V_i^c$ with respect to $\upsilon$ is by the Chain rule given by $\frac{\partial g_i(\boldsymbol{M})}{\partial \upsilon} = trace\left\{ \left( \frac{\partial g_i(\boldsymbol{M})}{\partial \boldsymbol{M}} \right)^\top \frac{\partial \boldsymbol{M}}{\partial \upsilon} \right\}$. Note that $g_i(\boldsymbol{M}) = \boldsymbol{E}_i^\top \boldsymbol{S}^c$, where $\boldsymbol{E}_i = \boldsymbol{E}_{iu} + (1-\kappa)\boldsymbol{E}_{iv}$, $\boldsymbol{E}_{iu}^\top = \left( \boldsymbol{e}_{3,i+2}^\top, \boldsymbol{e}_{3,i+2}^\top, \boldsymbol{0}_3^\top \right)$ and $\boldsymbol{E}_{iv}^\top = \left( \boldsymbol{0}_6^\top, \boldsymbol{e}_{3,i+2}^\top \right)$, and $\boldsymbol{e}_{m,k}$ is the single-entry $m$-vector with one at position $k$ and zeros elsewhere. From writing $g_i(\boldsymbol{M}) = \boldsymbol{E}_i^\top \boldsymbol{M}^{-1}\boldsymbol{\eta}$, it follows that $\frac{\partial g_i(\boldsymbol{M})}{\partial \boldsymbol{M}} = -\left(\boldsymbol{M}^{-1}\right)^\top \boldsymbol{E}_i \boldsymbol{\eta}^\top \left(\boldsymbol{M}^{-1}\right)^\top$, thus $\left( \frac{\partial g_i(\boldsymbol{M})}{\partial \boldsymbol{M}} \right)^\top = -\boldsymbol{S}^c \boldsymbol{E}_i^\top \boldsymbol{M}^{-1}$. □

## Appendix D. Details on the Disease–free State of the UVEIQR-Opinion Model

We provide a formula for each of the nine elements of the susceptibles states of the disease-free equilibrium $\boldsymbol{X}^c$ (19a) of the UVEIQR-Opinion Model (14), i.e. the expression of $\boldsymbol{S}^c$ given in matrix notation by Equation (19b) is developed here.

## References


1. Morens, D.M.; Fauci, A.S. Emerging pandemic diseases: how we got to COVID-19. *Cell* **2020**, *182*, 1077–1092.
2. Neiderud, C.J. How urbanization affects the epidemiology of emerging infectious diseases. *Infection Ecology & Epidemiology* **2015**, *5*, 27060.
3. Smith, K.F.; Acevedo-Whitehouse, K.; Pedersen, A.B. The role of infectious diseases in biological conservation. *Animal Conservation* **2009**, *12*, 1–12.
4. Woolhouse, M.E.; Gowtage-Sequeria, S. Host range and emerging and reemerging pathogens. *Emerging Infectious Diseases* **2005**, *11*, 1842.
5. Lee, B.; Ibrahim, S.A.; Zhang, T.; others. Mobile Apps Leveraged in the COVID-19 Pandemic in East and South-East Asia: Review and Content Analysis. *JMIR mHealth and uHealth* **2021**, *9*, e32093.
6. Liu, S.; Li, J.; Liu, J.; others. Leveraging Transfer Learning to Analyze Opinions, Attitudes, and Behavioral Intentions Toward COVID-19 Vaccines: Social Media Content and Temporal Analysis. *Journal of Medical Internet Research* **2021**, *23*, e30251.
7. Chou, W.Y.S.; Budenz, A. Considering emotion in COVID-19 vaccine communication: addressing vaccine hesitancy and fostering vaccine confidence. *Health Communication* **2020**, *35*, 1718–1722.
8. Mheidly, N.; Fares, J. Leveraging media and health communication strategies to overcome the COVID-19 infodemic. *Journal of Public Health Policy* **2020**, *41*, 410–420.
9. Prieto Curiel, R.; González Ramírez, H. Vaccination strategies against COVID-19 and the diffusion of anti-vaccination views. *Scientific Reports* **2021**, *11*, 1–13.
10. Pires, M.A.; Oestereich, A.L.; Crokidakis, N. Sudden transitions in coupled opinion and epidemic dynamics with vaccination. *Journal of Statistical Mechanics: Theory and Experiment* **2018**, *2018*, 053407.
11. Pires, M.A.; Crokidakis, N. Dynamics of epidemic spreading with vaccination: impact of social pressure and engagement. *Physica A: Statistical Mechanics and its Applications* **2017**, *467*, 167–179.
12. Rapaka, R.R.; Hammershaimb, E.A.; Neuzil, K.M. Are Some COVID-19 Vaccines Better Than Others? Interpreting and Comparing Estimates of Efficacy in Vaccine Trials. *Clinical Infectious Diseases* **2022**, *74*, 352–358.
13. Remmel, A.; others. COVID vaccines and safety: what the research says. *Nature* **2021**, *590*, 538–540.
14. Ledford, H.; others. COVID vaccines and blood clots: five key questions. *Nature* **2021**, *592*, 495–496.
15. Bonnevie, E.; Gallegos-Jeffrey, A.; Goldbarg, J.; Byrd, B.; Smyser, J. Quantifying the rise of vaccine opposition on Twitter during the COVID-19 pandemic. *Journal of Communication in Healthcare* **2021**, *14*, 12–19.
16. Cotfas, L.A.; Delcea, C.; Roxin, I.; Ioanăş, C.; Gherai, D.S.; Tajariol, F. The longest month: Analyzing covid-19 vaccination opinions dynamics from tweets in the month following the first vaccine announcement. *IEEE Access* **2021**, *9*, 33203–33223.
17. Muric, G.; Wu, Y.; Ferrara, E.; others. COVID-19 Vaccine Hesitancy on Social Media: Building a Public Twitter Data Set of Antivaccine Content, Vaccine Misinformation, and Conspiracies. *JMIR Public Health and Surveillance* **2021**, *7*, e30642.
18. Eibensteiner, F.; Ritschl, V.; Nawaz, F.A.; Fazel, S.S.; Tsagkaris, C.; Kulnik, S.T.; Crutzen, R.; Klager, E.; Völkl-Kernstock, S.; Schaden, E.; others. People's willingness to vaccinate against COVID-19 despite their safety concerns: Twitter poll analysis. *Journal of medical Internet research* **2021**, *23*, e28973.
19. Burki, T. The online anti-vaccine movement in the age of COVID-19. *The Lancet Digital Health* **2020**, *2*, e504–e505.

20. Jamison, A.M.; Broniatowski, D.A.; Dredze, M.; Sangraula, A.; Smith, M.C.; Quinn, S.C. Not just conspiracy theories: Vaccine opponents and proponents add to the COVID-19 'infodemic'on Twitter. *Harvard Kennedy School Misinformation Review* **2020**, *1*.
21. Alvarez-Zuzek, L.G.; La Rocca, C.E.; Iglesias, J.R.; Braunstein, L.A. Epidemic spreading in multiplex networks influenced by opinion exchanges on vaccination. *PloS One* **2017**, *12*, e0186492.
22. Tyson, R.C.; Hamilton, S.D.; Lo, A.S.; Baumgaertner, B.O.; Krone, S.M. The timing and nature of behavioural responses affect the course of an epidemic. *Bulletin of Mathematical Biology* **2020**, *82*, 1–28.
23. She, B.; Liu, J.; Sundaram, S.; Paré, P.E. On a Networked SIS Epidemic Model with Cooperative and Antagonistic Opinion Dynamics. *IEEE Transactions on Control of Network Systems* **2022**. doi:10.1109/TCNS.2022.3145748.
24. Boucekkine, R.; Carvajal, A.; Chakraborty, S.; Goenka, A. The economics of epidemics and contagious diseases: An introduction. *Journal of Mathematical Economics* **2021**.
25. McAdams, D. The blossoming of economic epidemiology. *Annual Review of Economics* **2021**, *13*, 539–570.
26. Nardin, L.G.; Miller, C.R.; Ridenhour, B.J.; Krone, S.M.; Joyce, P.; Baumgaertner, B.O. Planning horizon affects prophylactic decision-making and epidemic dynamics. *PeerJ* **2016**, *4*, e2678.
27. Gersovitz, M. Mathematical epidemiology and welfare economics. In *Modeling the interplay between human behavior and the spread of infectious diseases*; Springer, 2013; pp. 185–202.
28. Valle, S.Y.D.; Mniszewski, S.M.; Hyman, J.M. Modeling the impact of behavior changes on the spread of pandemic influenza. In *Modeling the interplay between human behavior and the spread of infectious diseases*; Springer, 2013; pp. 59–77.
29. Perra, N.; Balcan, D.; Gonçalves, B.; Vespignani, A. Towards a characterization of behavior-disease models. *PloS One* **2011**, *6*, e23084.
30. Fenichel, E.P.; Castillo-Chavez, C.; Ceddia, M.G.; Chowell, G.; Parra, P.A.G.; Hickling, G.J.; Holloway, G.; Horan, R.; Morin, B.; Perrings, C.; others. Adaptive human behavior in epidemiological models. *Proceedings of the National Academy of Sciences* **2011**, *108*, 6306–6311.
31. Moore, T.W.; Finley, P.D.; Linebarger, J.M.; Outkin, A.V.; Verzi, S.J.; Brodsky, N.S.; Cannon, D.C.; Zagonel, A.A.; Glass, R.J. Extending Opinion Dynamics to Model Public Health Problems and Analyze Public Policy Interventions. In *Proceedings of the 29th Intl Conf of the System Dynamics Society*; Citeseer-NECSI ICCS: Sandia National Laboratories, USA, 2011; Vol. 1, pp. 1–15.
32. Funk, S.; Gilad, E.; Watkins, C.; Jansen, V.A. The spread of awareness and its impact on epidemic outbreaks. *Proceedings of the National Academy of Sciences* **2009**, *106*, 6872–6877.
33. Basu, S.; Chapman, G.B.; Galvani, A.P. Integrating epidemiology, psychology, and economics to achieve HPV vaccination targets. *Proceedings of the National Academy of Sciences* **2008**, *105*, 19018–19023.
34. Epstein, J.M.; Parker, J.; Cummings, D.; Hammond, R.A. Coupled contagion dynamics of fear and disease: mathematical and computational explorations. *PloS One* **2008**, *3*, e3955.
35. Ferguson, N. Capturing human behaviour. *Nature* **2007**, *446*, 733–733.
36. Kawachi, I. Why social epidemiology? *Australasian Epidemiologist* **2000**, *7*, 5–6.
37. Xuan, W.; Ren, R.; Paré, P.E.; Ye, M.; Ruf, S.; Liu, J. On a network SIS model with opinion dynamics. *IFAC-PapersOnLine* **2020**, *53*, 2582–2587.
38. She, B.; Leung, H.C.; Sundaram, S.; Paré, P.E. Peak Infection Time for a Networked SIR Epidemic with Opinion Dynamics, 2021. doi:arXiv:2109.14135.
39. Liang, D.; Yi, B.; Xu, Z. Opinion dynamics based on infectious disease transmission model in the non-connected context of Pythagorean fuzzy trust relationship. *Journal of the Operational Research Society* **2021**, *72*, 2783–2803.
40. Oestereich, A.L.; Pires, M.A.; Crokidakis, N. Three-state opinion dynamics in modular networks. *Physical Review E* **2019**, *100*, 032312.
41. Bhowmick, S.; Panja, S. Influence of opinion dynamics to inhibit epidemic spreading over multiplex network. *IEEE Control Systems Letters* **2020**, *5*, 1327–1332.
42. Jankowski, R.; Chmiel, A. Role of Time Scales in the Coupled Epidemic-Opinion Dynamics on Multiplex Networks. *Entropy* **2022**, *24*, 105.
43. Mahmood, M.; Khan, M.F.; Hasrat, M.N.; Richwagen, N.; others. Transmission frequency of COVID-19 through pre-symptomatic and asymptomatic patients in AJK: a report of 201 cases. *Virology Journal* **2021**, *18*, 1–8.
44. Johansson, M.A.; Quandelacy, T.M.; Kada, S.; Prasad, P.V.; Steele, M.; Brooks, J.T.; Slayton, R.B.; Biggerstaff, M.; Butler, J.C. SARS-CoV-2 transmission from people without COVID-19 symptoms. *JAMA Network Open* **2021**, *4*, e2035057–e2035057.
45. Kraemer, M.U.; Pybus, O.G.; Fraser, C.; Cauchemez, S.; Rambaut, A.; Cowling, B.J. Monitoring key epidemiological parameters of SARS-CoV-2 transmission. *Nature Medicine* **2021**, *27*, 1854–1855.
46. Salzberger, B.; Buder, F.; Lampl, B.; Ehrenstein, B.; Hitzenbichler, F.; Holzmann, T.; Schmidt, B.; Hanses, F. Epidemiology of SARS-CoV-2. *Infection* **2021**, *49*, 233–239.
47. Homma, Y.; Katsuta, T.; Oka, H.; Inoue, K.; Toyoshima, C.; Iwaki, H.; Yamashita, Y.; Shinomiya, H. The incubation period of the SARS-CoV-2 B1. 1.7 variant is shorter than that of other strains. *Journal of Infection* **2021**, *83*, e15–e17.

48. Hu, X.; Ni, W.; Wang, Z.; Ma, G.; Pan, B.; Dong, L.; Gao, R.; Jiang, F. The distribution of SARS-CoV-2 contamination on the environmental surfaces during incubation period of COVID-19 patients. *Ecotoxicology and Environmental Safety* **2021**, *208*, 111438.
49. Kim, S.E.; Jeong, H.S.; Yu, Y.; Shin, S.U.; Kim, S.; Oh, T.H.; Kim, U.J.; Kang, S.J.; Jang, H.C.; Jung, S.I.; others. Viral kinetics of SARS-CoV-2 in asymptomatic carriers and presymptomatic patients. *International Journal of Infectious Diseases* **2020**, *95*, 441–443.
50. Jiang, X.; Rayner, S.; Luo, M.H. Does SARS-CoV-2 has a longer incubation period than SARS and MERS? *Journal of medical virology* **2020**, *92*, 476–478.
51. Hussain, T.; Ozair, M.; Ali, F.; ur Rehman, S.; Assiri, T.A.; Mahmoud, E.E. Sensitivity analysis and optimal control of COVID-19 dynamics based on SEIQR model. *Results in Physics* **2021**, *22*, 1–11.
52. Gerberry, D.J.; Milner, F.A. An SEIQR model for childhood diseases. *Journal of Mathematical Biology* **2009**, *59*, 535–561.
53. Jumpen, W.; Wiwatanapataphee, B.; Wu, Y.; Tang, I. A SEIQR model for pandemic influenza and its parameter identification. *International Journal of Pure and Applied Mathematics* **2009**, *52*, 247–265.
54. Tovissodé, C.F.; Doumatè, J.T.; Glèlè Kakaï, R. A Hybrid Modeling Technique of Epidemic Outbreaks with Application to COVID-19 Dynamics in West Africa. *Biology* **2021**, *10*, 365.
55. Iboi, E.A.; Sharomi, O.O.; Ngonghala, C.N.; Gumel, A.B. Mathematical modeling and analysis of COVID-19 pandemic in Nigeria, 2020.
56. Taboe, H.B.; Salako, K.V.; Tison, J.M.; Ngonghala, C.N.; Kakaï, R.G. Predicting COVID-19 spread in the face of control measures in West Africa. *Mathematical Biosciences* **2020**, *328*, 108431.
57. Hethcote, H.; Zhien, M.; Shengbing, L. Effects of quarantine in six endemic models for infectious diseases. *Mathematical Biosciences* **2002**, *180*, 141–160.
58. Iachini, T.; Frassinetti, F.; Ruotolo, F.; Sbordone, F.L.; Ferrara, A.; Arioli, M.; Pazzaglia, F.; Bosco, A.; Candini, M.; Lopez, A.; others. Social distance during the COVID-19 pandemic reflects perceived rather than actual risk. *International Journal of Environmental Research and Public Health* **2021**, *18*, 5504.
59. Welsch, R.; Wessels, M.; Bernhard, C.; Thönes, S.; von Castell, C. Physical distancing and the perception of interpersonal distance in the COVID-19 crisis. *Scientific Reports* **2021**, *11*, 1–9.
60. Chevalier-Cottin, E.P.; Ashbaugh, H.; Brooke, N.; Gavazzi, G.; Santillana, M.; Burlet, N.; Tin Tin Htar, M. Communicating benefits from vaccines beyond preventing infectious diseases. *Infectious Diseases and Therapy* **2020**, *9*, 467–480.
61. Bloom, D.E.; Cadarette, D.; Ferranna, M. The societal value of vaccination in the age of COVID-19. *American Journal of Public Health* **2021**, *111*, 1049–1054.
62. Andersson, O.; Campos-Mercade, P.; Meier, A.N.; Wengström, E. Anticipation of COVID-19 vaccines reduces willingness to socially distance. *Journal of Health Economics* **2021**, *80*, 1–10.
63. Van den Driessche, P.; Watmough, J. Reproduction numbers and sub-threshold endemic equilibria for compartmental models of disease transmission. *Mathematical Biosciences* **2002**, *180*, 29–48.
64. Hodgson, S.H.; Mansatta, K.; Mallett, G.; Harris, V.; Emary, K.R.; Pollard, A.J. What defines an efficacious COVID-19 vaccine? A review of the challenges assessing the clinical efficacy of vaccines against SARS-CoV-2. *The lancet infectious diseases* **2021**, *21*, e26–e35.
65. Hall, V.J.; Foulkes, S.; Saei, A.; Andrews, N.; Oguti, B.; Charlett, A.; Wellington, E.; Stowe, J.; Gillson, N.; Atti, A.; others. COVID-19 vaccine coverage in health-care workers in England and effectiveness of BNT162b2 mRNA vaccine against infection (SIREN): a prospective, multicentre, cohort study. *The Lancet* **2021**, *397*, 1725–1735.
66. Davies, N.G.; Klepac, P.; Liu, Y.; Prem, K.; Jit, M.; Eggo, R.M. Age-dependent effects in the transmission and control of COVID-19 epidemics. *Nature medicine* **2020**, *26*, 1205–1211.
67. Omori, R.; Matsuyama, R.; Nakata, Y. The age distribution of mortality from novel coronavirus disease (COVID-19) suggests no large difference of susceptibility by age. *Scientific reports* **2020**, *10*, 1–9.
68. Monod, M.; Blenkinsop, A.; Xi, X.; Hebert, D.; Bershan, S.; Tietze, S.; Baguelin, M.; Bradley, V.C.; Chen, Y.; Coupland, H.; others. Age groups that sustain resurging COVID-19 epidemics in the United States. *Science* **2021**, *371*, eabe8372.
69. Sadarangani, M.; Raya, B.A.; Conway, J.M.; Iyaniwura, S.A.; Falcao, R.C.; Colijn, C.; Coombs, D.; Gantt, S. Importance of COVID-19 vaccine efficacy in older age groups. *Vaccine* **2021**, *39*, 2020–2023.
70. Bouzid, D.; Visseaux, B.; Kassasseya, C.; Daoud, A.; Fémy, F.; Hermand, C.; Truchot, J.; Beaune, S.; Javaud, N.; Peyrony, O.; others. Comparison of patients infected with Delta versus Omicron COVID-19 variants presenting to Paris emergency departments: a retrospective cohort study. *Annals of internal medicine* **2022**, *175*, 831–837.
71. Butt, A.A.; Dargham, S.R.; Tang, P.; Chemaitelly, H.; Hasan, M.R.; Coyle, P.V.; Kaleeckal, A.H.; Latif, A.N.; Loka, S.; Shaik, R.M.; others. COVID-19 disease severity in persons infected with the Omicron variant compared with the Delta variant in Qatar. *Journal of global health* **2022**, *12*.
72. Walter, E.B.; Talaat, K.R.; Sabharwal, C.; Gurtman, A.; Lockhart, S.; Paulsen, G.C.; Barnett, E.D.; Muñoz, F.M.; Maldonado, Y.; Pahud, B.A.; others. Evaluation of the BNT162b2 Covid-19 vaccine in children 5 to 11 years of age. *New England Journal of Medicine* **2022**, *386*, 35–46.
73. Castro, M.C.; Singer, B. Prioritizing COVID-19 vaccination by age. *Proceedings of the National Academy of Sciences* **2021**, *118*, 1–1.

74. Bubar, K.M.; Reinholt, K.; Kissler, S.M.; Lipsitch, M.; Cobey, S.; Grad, Y.H.; Larremore, D.B. Model-informed COVID-19 vaccine prioritization strategies by age and serostatus. *Science* **2021**, *371*, 916–921.
75. Shakoor, S.; Rao, A.; Shahid, N.; Yaqoob, A.; Samiullah, T.; Shakoor, S.; Latif, A.; Tabassum, B.; Khan, M.; Shahid, A.; others. Role of oral vaccines as an edible tool to prevent infectious diseases. *Acta Virol* **2019**, *63*, 245–252.
76. Seib, K.L.; Dougan, G.; Rappuoli, R. The key role of genomics in modern vaccine and drug design for emerging Infectious Diseases. *PLoS Genetics* **2009**, *5*, e1000612.
77. Shaw, L.B.; Schwartz, I.B. Enhanced vaccine control of epidemics in adaptive networks. *Physical Review E* **2010**, *81*, 1–5. doi:10.1103/physreve.81.046120.
78. Zanette, D.H.; Kuperman, M. Effects of immunization in small-world epidemics. *Physica A: Statistical Mechanics and its Applications* **2002**, *309*, 445–452. doi:10.1016/s0378-4371(02)00618-0.
79. Martcheva, M. *An Introduction to Mathematical Epidemiology*, 1st ed.; Vol. 61, *Texts in Applied Mathematics*, Springer New York, 2015.
80. May, R.M. *Stability and Complexity in Model Ecosystems. (MPB-6) (Monographs in Population Biology)*; Princeton University Press, 1973.
81. Castillo-Chavez, C.; Feng, Z.; Huang, W. On the computation of $R_0$ and its role on global stability. *The IMA Volumes in Mathematics and Its Applications* **2002**, *125*, 229–250.
82. Cheng-Cheng, Zhu and Jiang, Zhu and Xiao-Lan Liu. Influence of spatial heterogeneous environment on long-term dynamics of a reaction-diffusion S VIR epidemic model with relapse. *Bulletin of the Polish Academy of Sciences: Technical Sciences* **2019**, *16*, 5897–5922. doi:10.3934/mbe.2019295.
83. Smith, H.L. *Monotone dynamical systems: An introduction to the theory of competitive and cooperative systems*; Mathematical Surveys and Monographs, AMS, 2008.
84. Krasnoselskii, M.A. *Positive Solutions of Operator Equations*; Noordhoff. Groningen, 1964.
85. Hethcote, H.W.; Thieme, H.R. Stability of the Endemic Equilibrium in Epidemic Models with Subpopulations. *Mathematical Biosciences* **1985**, *75*, 205–227.
86. Mazenc, F. Strict Lyapunov functions for time-varying systems. *Automatica* **2003**, *39*, 349–353.
87. Farkas, B.; Wegner, S.A. Variations on Barbălat's lemma. *The American Mathematical Monthly* **2016**, *123*, 825–830.